TAMPEREEN TEKNILLINEN YLIOPISTO
TAMPERE UNIVERSITY OF TECHNOLOGY

SAIF ULLAH KHAN

THE OPERATION OF TUT SOLAR PHOTOVOLTAIC POWER RESEARCH PLANT

Master of Science thesis

Examiner: prof. Seppo Valkealahti
Examiner and topic approved by the Faculty Council of the Faculty of Electrical Engineering on 4th February 2015

ABSTRACT

SAIF ULLAH KHAN: The operation of TUT solar photovoltaic power research plant
Tampere University of technology
Master of Science Thesis, 47 pages, 1 Appendix page
February 2016
Master's Degree Programme in Electrical Engineering
Major: Smart Grids
Examiner: Professor Seppo Valkealahti

Keywords: PV module, ambient temperature, irradiance

Photovoltaic power production has a large potential when it comes to converting solar energy into electrical energy. This is the reason that the number of photovoltaic power plants in Finland is on the rise. This increasing trend makes it very essential to study the effects of various environmental factors on the operation of photovoltaic power plants. Factors such as ambient temperature, wind speed, diffuse radiation, global radiation and humidity are very important to the operation of photovoltaic power plants. These factors directly or indirectly effect the power production and therefore determine the feasibility of a photovoltaic power plant in a particular environment.

Therefore, it was important to study the profiles for the above mentioned environmental factors from the research power plant located in Tampere University of Technology, Tampere, Finland. The annual and seasonal profiles from January 2014 to December 2014 were studied and analyzed. The measurements were taken using the state of the art data acquisition system installed at the test facility. The effect on module temperature and irradiance was also studied.

It was concluded from the results that humidity remained highest during the winter months because of heavy cloud cover. This cloud cover was also responsible for the fact that global solar radiation was almost equal to diffused solar radiation during winter time. Thus, for maximum production and working efficiency it was essential to ensure that the diffuse radiation component was also harvested by the photovoltaic power plants. Wind speed more or less remained the same over the course of a year with the highest value during the autumn period in months of September and October. The maximum average value recorded for ambient temperature was during the summer period. The study revealed that for the maximum working efficiency of a photovoltaic power plant the behavior of various environmental factors such as wind speed, global and diffuse radiation, humidity and ambient temperature must be taken into account.

PREFACE

This thesis is written as part of the completion of Master of Science (Technology) degree in Electrical Engineering. The work was completed at the Department of Electrical Engineering at Tampere University of Technology. It was supervised and examined by Professor Seppo Valkealahti. I would like to thank my supervisor for providing me with this great opportunity and for his ideas and guidance throughout the work. The ideas provided by him have been a corner stone in making this thesis an effective piece of work.

Secondly, I would also thank Mr. Kari Lappalainen for his help and support. I am also thankful to the Department of Electrical Engineering specially the Smart Grids research group for providing me with an excellent learning and working environment. I would like to thank my family and friends for their support. In the end I would like to dedicate this work to my dad who has been a constant source of motivation and encouragement behind every decision I have made in this life.

Tampere, (18.11.2016)

Saif Ullah Khan

CONTENTS

LIST OF FIGURES

List of Symbols and abbreviations

Symbols

A	ideality factor of a PV cell
c	speed of light
E_C	conduction band energy
E_G	bandgap energy
E_P	energy of photon
E_V	valence band energy
f	frequency of light
h	Plank's constant
h_{smax}	highest elevation of the sun
h_s	solar altitude
I_0	diode saturation current
I_{MPP}	Current at the maximum power point
I_{SC}	short circuit current
K	temperature in kelvin
k	Boltzmann's constant
L	distance between the sensors
m	mass
P_{MPP}	Power at the maximum power point
q	electronic charge
R_s	series resistance
R_{sh}	shunt resistance
t_f	transit time in the forward direction
t_r	transit time in the reverse direction
V_{MPP}	Voltage at the maximum power point
V_{oc}	open circuit voltage
V_W	velocity of wind
γ_s	solar azimuth
δ	solar declination
λ	wavelength of light
φ	latitude of a particular location
ω_S	hour angle

Abbreviations

AC	Alternating Current
AM	Air Mass
AWS	Automatic Weather Station
CB	Conduction Band
DC	Direct Current
FMI	Finnish Meteorological Institute
IR	Infrared
ISO	International Organization for Standardization
LED	Light Emitting Diode

MATLAB	Matrix Laboratory, a proprietary programming language which allows plotting of functions and data for better visualization.
MPP	Maximum Power Point
PV	Photovoltaic
STC	Standard Test Conditions
TUT	Tampere University of Technology
URL	Uniform Resource Locator
UV	Ultra Violet
VB	Valence Band
2D	Two Dimensional
3D	Three Dimensional

1. INTRODUCTION

Energy has been one of the most important resources used for economic development since the beginning of mankind. The fact that the World population is expected to get double by the middle of the 21st century has a direct effect on the primary energy requirements which are expected to increase by approximately three folds by the year 2050 and five folds by the year 2100 [1]. The extensive use of fossil fuels to meet the energy demands has led to the degradation of earth's environment and its atmosphere. In order to protect our environment there is a need to switch to clean, sustainable, efficient and eco-friendly ways of energy and power production in the future.

Since ancient times the sun has been worshipped as a life giver to our planet. Energy from the sun also known as solar energy is a clean, natural and renewable source of energy which is available to almost all parts of the World. The energy supply from the sun is enormous. In ninety minutes, enough sunlight strikes the earth to provide the entire planet's energy needs for one year [2]. The approximate measure of this solar energy incident on earth's surface is 1.5 x 10^{18} kWh/year. Solar energy constant which is a measure of the density of the power radiated from the sun is 1.373 kW/m^2 [1]. Solar energy is converted to electrical energy by a phenomena known as the photovoltaic (PV) effect. The devices used in this process are known as solar cells. The amount of electric current generated by a solar cell depends on factors such as efficiency, surface area (size), type and light intensity.

The history of photovoltaics takes us back over 150 years when in 1839, Alexander-Edmund Becquerel observed that certain electrical currents arose from certain light-induced chemical reactions thus leading to the discovery of photovoltaic effect. This was further strengthened by Willoughby Smith in 1873 with the discovery of photoconductivity of selenium. In 1916, the experimental proof of the photoelectric effect was provided by Robert Millikan for the first time. The development of the first solid state devices led to the birth of the photovoltaic technology in 1954 in the United States. The first solar cell which was capable of converting the sun's energy into electrical power was developed at Bell Labs by Daryl Chapin, Calvin Fuller and Gerald Pearson. The efficiency of this solar cell was 4% and later on an efficiency of 11% was achieved by Bell Labs. Solar cells found their first application in the Vanguard 1 satellite when a small array was installed to power the radios on the satellite. Photovoltaic cells with efficiencies of 8%, 9%, 10% and 14% were developed in 1957, 1958, 1959 and 1960 respectively by Hoffman electronics adding to the milestones achieved by photovoltaic technology [3].

The detailed balance limit which defines the maximum theoretical power conversion efficiency of a single pn junction was proposed in 1961 by William Shockley and Hans Queisser. The experiments concluded that the maximum power conversion efficiency of a single pn junction solar cell with a bandgap of 1.4 eV and solar radiation similar to 6000 K blackbody radiation is 33.7% [4]. The Institute of Energy Conversion established in 1972 at the University of Delaware was the first laboratory dedicated to PV research and development. Organizations such as NASA in the USA and NASDA in Japan are working on PV systems which would find their application in space shuttles [3].

One of the main advantages of photovoltaic power generation is that it is environment friendly and involves zero emissions when compared to the conventional sources of power generation which involve the use of fossil fuels and are a major factor behind global warming and environmental degradation. Photovoltaic power generation is reliable and involves no moving parts. The operation and maintenance costs are low. These systems are easily installed because they are modular [5].

Solar energy is still not utilized to its full potential because of some concerns. One of the major concern is that maximum solar energy can only be harnessed during daytime when the conditions are sunny. The variation in the amount of sunlight over the course of different seasons is also a major drawback. For example cloud cover reduces the amount of power produced by a photovoltaic module. PV systems produce direct current (DC) power which has to be inverted to alternating current (AC) for residential or commercial applications [5].

The Department of Electrical Engineering at the Tampere University of Technology has designed and installed a PV power station for research purposes. The power plant comprises of 69 NP195GKg solar photovoltaic modules located on the rooftop of the department. The primary objective of this power plant is to study the effect of various environmental parameters on the operation of photovoltaic power generator. It is also used for the testing and evaluation of different power electronic components and systems [6].

The main objective of this thesis is to study the operation of the PV power plant installed at Tampere University of Technology (TUT). The measurements for parameters such as ambient temperature, diffused solar radiation, global solar radiation, humidity, wind speed and wind direction have been taken and their behavior has been studied for the year 2014. CMP22 and CMP21 are the pyranometers used to measure global and diffused solar radiation respectively. HMP155 measures temperature and humidity and WS425 measures wind speed and direction. The measurements are studied using simulations in MATLAB computer software. The annual variations of these climatic parameters and their effect on module irradiance and temperature is studied through these simulations. The study has also been used to determine the correlation between these climatic parameters.

The following is the structure of this thesis. Chapter 2 discusses the basics of solar energy. The fundamentals of solar radiation and the phenomena of solar declination is also studied in this chapter. This chapter also briefly discusses the PV cell and PV power plants. In chapter 3 various climatic parameters which effect the operation of PV power plants are introduced and briefly discussed. These parameters include global radiation, diffused radiation, ambient temperature, humidity and wind speed and direction. Chapter 4 throws light on the research PV power plant installed at TUT. In this chapter the configuration and layout of the plant is briefly explained along with the different sensors used for data measurement. The advanced data acquisition system is also explained as part of this chapter. In chapter 5 the complete analysis of the measured data is done with regard to the thesis. It includes analysis of annual and seasonal variation in the measured data for different climatic parameters. This chapter also briefly discusses the correlation between these climatic parameters. Finally, in chapter 6 the conclusions are discussed.

2. ENERGY FROM THE SUN

Careful assessment of solar radiation at a particular site is a key factor in the design of a photovoltaic system. This chapter outlines the properties of solar radiation on Earth. First, the astronomical relationship between the Sun and the Earth would be described along with the phenomena of solar declination which characterizes the apparent motion of the Sun. PV cells and PV systems would also be described as they are the building blocks of PV power plants which is the main focus of this thesis.

2.1 Sun and Earth

The amount of energy which the mankind utilizes is well over a 1000 times less than the amount of solar energy that reaches the surface of the Earth. The source of this energy which is the Sun converts hydrogen nuclei into helium nuclei thus releasing energy. Energy is released because the mass of the helium nuclei produced is less than that of the hydrogen nuclei. This process is also known as nuclear fusion and is governed by the following equation

$$E = mc^2. \tag{2.1}$$

This arises the fact that solar energy is fundamentally nuclear energy produced by the reactor known as Sun. The output of this gigantic nuclear reactor is roughly 10^{17} more than the thermal output of a 1200 MW nuclear power plant. There is no danger to humankind from this great nuclear reactor as it is at a very safe distance from Earth [7].

At a mean distance of 149.6 million km the Earth rotates around the Sun once per year in a slightly elliptical orbit. To a good approximation, the Sun acts as a perfect emitter of radiation which is the reason solar radiation is distributed evenly in all directions thus coining the term solar constant. Solar constant is defined as the irradiance at the outer edge of the Earth's atmosphere at a plane that is perpendicular to the direction of the Sun. It averages at 1367±2 W/m^2 with a variation of minimum 1322 W/m^2 to a maximum 1414 W/m^2. The variation is due to the slightly elliptical nature of the Earth's orbit [7].

The Earth's environment is having dire consequences due to the heavy usage of fossil fuels as a source of energy. It is the need of the hour to capture this large influx of energy from the Sun. This will ensure environment friendly energy usage along with powering human endeavours [7].

2.2 Solar declination

The variation in solar radiation over the course of a year at a location is due to the presence of Earth's axis at an angle of ±23.45˚ relative to the plane of Earth's path around the Sun. This is called ecliptic [8]. In fact, the Sun's rays come from different directions relative to the equatorial plane as the year passes. During the winter months the Earth's axis is inclined away from the Sun when compared to the summer months when it is inclined towards it. This inclination of the Earth's axis towards the Sun is known as solar declination δ and is given in radians by the following equation [7]

$$\delta = \pi \frac{23.45}{180} \sin\left(2\pi \frac{284 + n}{365}\right). \tag{2.2}$$

In the above equation 'n' represents the number of day in the year (n = 32 on 1st February) [5]. Figure 2.1 depicts the annual solar declination δ with the days numbered from 1 to 365

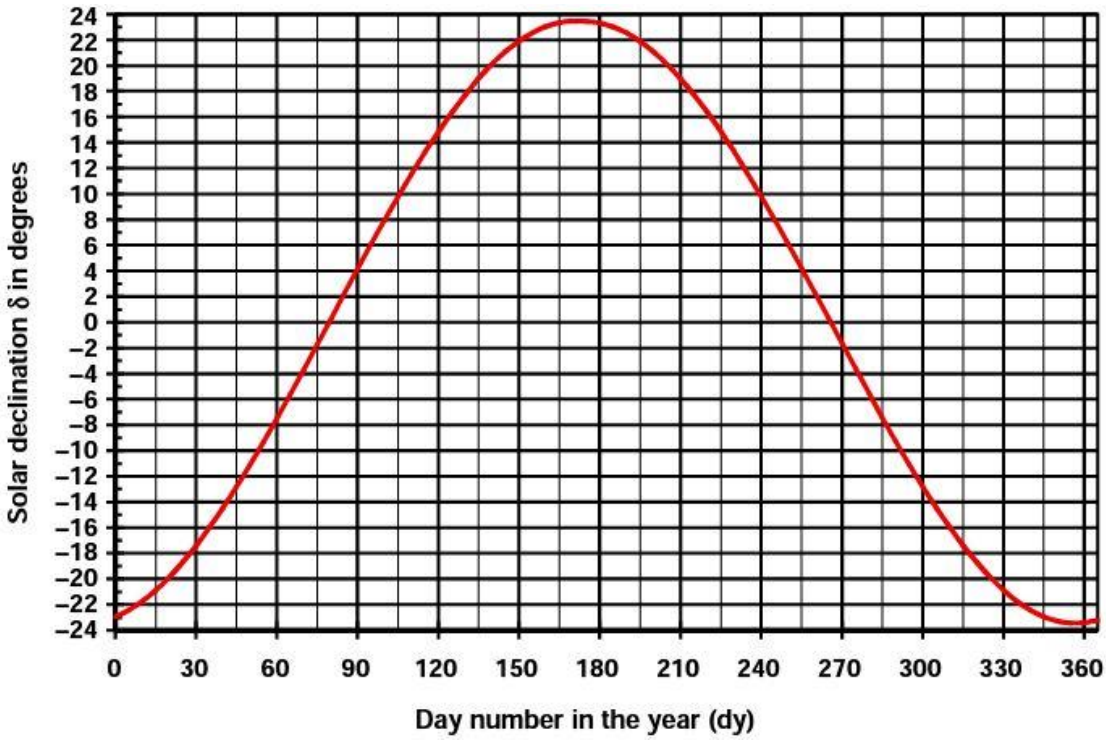

Figure 2.1 *Annual solar declination [7].*

The highest elevation of the Sun h_{smax} at noon is not constant during the year. Instead it depends on the solar declination. For example, in the northern hemisphere at a location with a latitude φ the highest elevation of the Sun is given by the equation [7]

$$h_{smax} = 90° - \varphi + \delta. \tag{2.3}$$

In this equation, h_{smax} is the maximum elevation of the Sun, φ is the latitude of a particular location and δ is the solar declination.

The maximum value of the solar declination is ±23.45˚. In the northern hemisphere solar declination achieves the value of 23.45˚ on the 21st of June which is also called the summer solstice and it reaches the value of -23.45˚ on the 21st of December which is known as the winter solstice. In the southern hemisphere this is completely opposite and the summer solstice occurs on 21st December and the winter solstice on 21st June. The value of solar declination is 0˚ on the equinoxes. Vernal equinox occurs on the 21st of March whereas autumnal equinox occurs on the 23rd of September. This can also be seen in the figure 2.2 below [7]

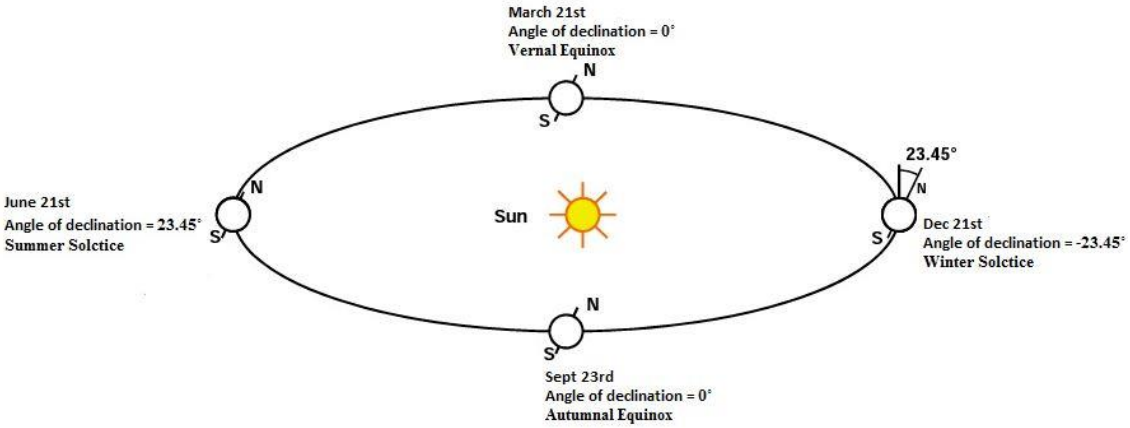

Figure 2.2 *Motion of earth around the sun and position of earth's axis around the year [4].*

Apparent motion of the sun is an important factor which should be taken into consideration when evaluating the performance of a photovoltaic power plant at a specific location. The mean deviation in mean distance in this orbit which is close in shape to a circle is less than two percent [8]. In order to calculate the Sun's path, the hour angle ω_S which is known as the angle between the local longitude coordinate of a specific location and the latitude coordinate from which the Sun is presently passing through the meridian. The following equation is used to calculate the hour angle [7]

$$Hour\ angle, \omega_S = (ST - 12)\ 15^\circ\ . \tag{2.4}$$

The factor 15˚ comes from the fact that the Earth completes one revolution around its own axis every 24 hours. ST is the true solar time measured between (0-24 hours) at the particular location. Solar elevation h_s which is the elevation of the Sun above the horizontal plane and solar azimuth γ_s which is the angle between the connecting line to the Sun projected onto the horizontal plane from the south are given by the following equations [7]

$$\sin h_s = \sin\varphi \sin\delta + \cos\varphi \cos\delta \cos\omega_S \tag{2.5}$$

$$\sin\gamma_s = \frac{\cos\delta \sin\omega_S}{\cos h_s}. \tag{2.6}$$

The path of the Sun can be traced from these equations at any particular time and location. Figure 2.3 also describes the position of the sun with respect to solar altitude and solar azimuth from a reference point on Earth [7]

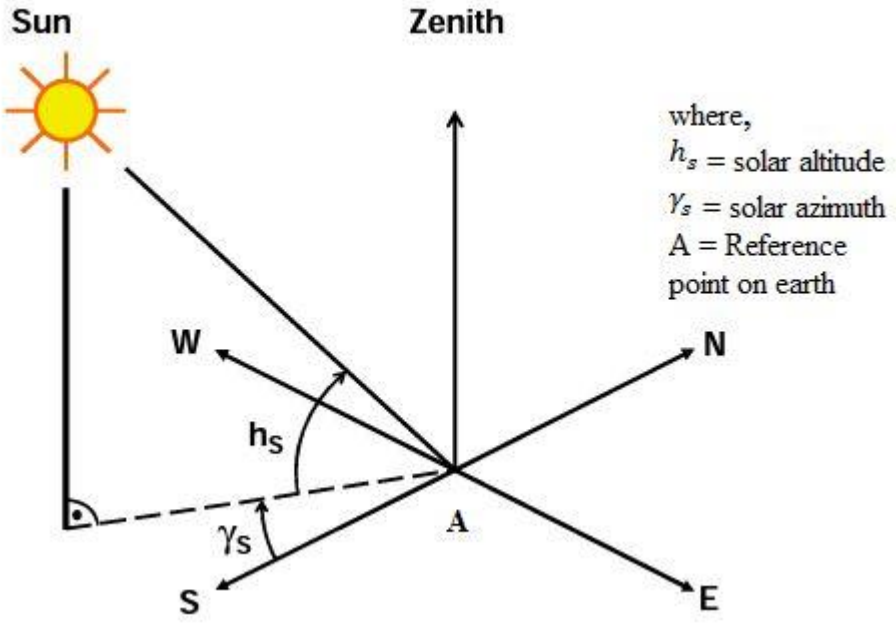

Figure 2.3 *Position of the sun from a reference point on earth using the solar azimuth and elevation angles [7].*

2.3 Fundamentals of solar radiation

Scientists have made continuous efforts over a period of centuries to understand the nature of light. During the last quarter of the 17th century Newton's theory that light is made up of small particles was widely accepted and was known as the mechanistic view of light. This was proved wrong by scientists Young and Fresnel when they discovered the effects of interference in light beams indicating that light was made up of waves. In 1860, light was defined as a spectrum of electromagnetic waves having different wavelengths by Maxwell in his theory of electromagnetic radiation. This debate was put to rest by Albert Einstein in 1905 when he explained the photovoltaic effect. It regarded electromagnetic radiation as both waves and particle. It proposed that light was made up of discrete particles or 'quanta' of energy called photons. It was concluded that electromagnetic radiation had a complementary nature known as particle-wave duality. It is described by the equation

$$E_P = hf = \frac{hc}{\lambda}. \tag{2.7}$$

In the above equation, f is the frequency of light, λ is the wavelength of the light, E_P is the energy of photons which come in packets. h is the Plank's constant which has a value of $6.626 \cdot 10^{34}$ Js and c is the speed of light $2.99792 \cdot 10^{8}$ m/s [9].

Electromagnetic radiation is generated by the thermal motion of charged particles in matter. It is also called thermal radiation. This leads to the fact that thermal radiation is emitted by all the matter which has a temperature greater than absolute zero. A blackbody is an ideal absorber and emitter of radiation. Figure 2.4 shows at three different temperatures the spectrum of a blackbody radiation [8].

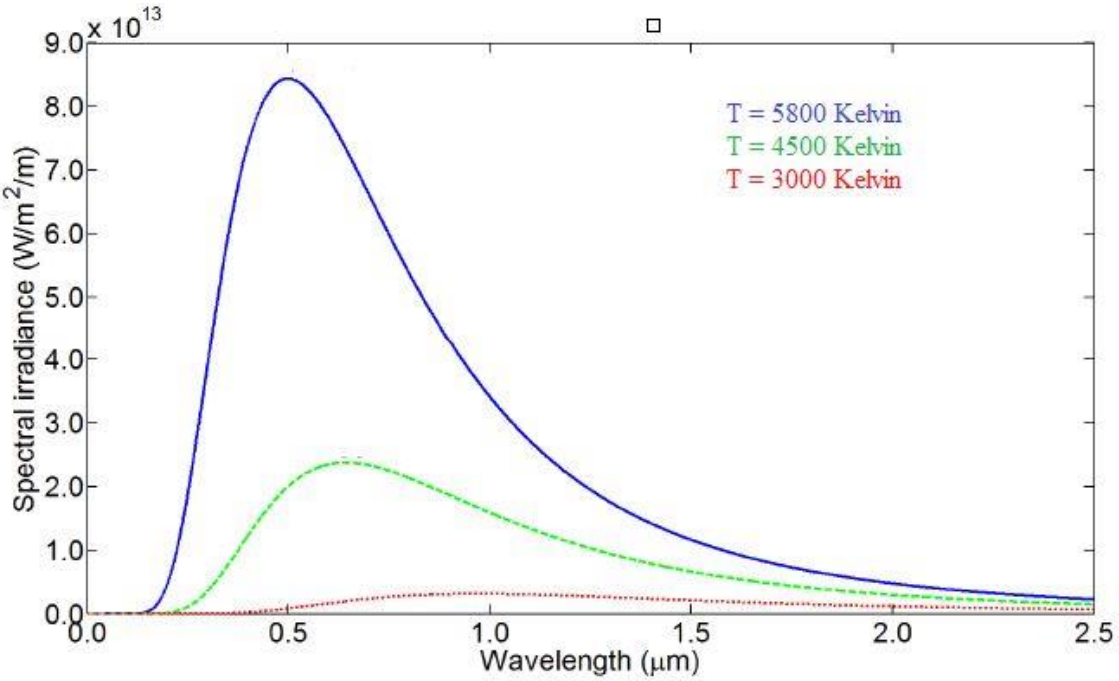

Figure 2.4 *Blackbody spectral intensity for three temperatures [8]*

It can be concluded from figure 2.4 that the higher the temperature of an object is the shorter is the wavelength of the maximum of the spectral irradiance. The upper most curve shows the spectral irradiance emitted from the surface of the Sun. The surface temperature of the Sun is approximately 5800 K.

The Sun acts as a perfect emitter of light at a temperature of approximately 5800 K. Figure 2.5 shows the spectral distribution of energy from the Sun. The figure shows a smooth curve which is common to a blackbody like the Sun. It shows that radiation from the Sun has a range from 0.2 μm to 2.0 μm with the peak value at 0.5 μm. Visible spectrum to the human eye is between 400 nm to 800 nm. Wavelengths shorter than 400 nm are called ultraviolet (UV) rays where as those longer than 800 nm are called infrared (IR) rays [10].

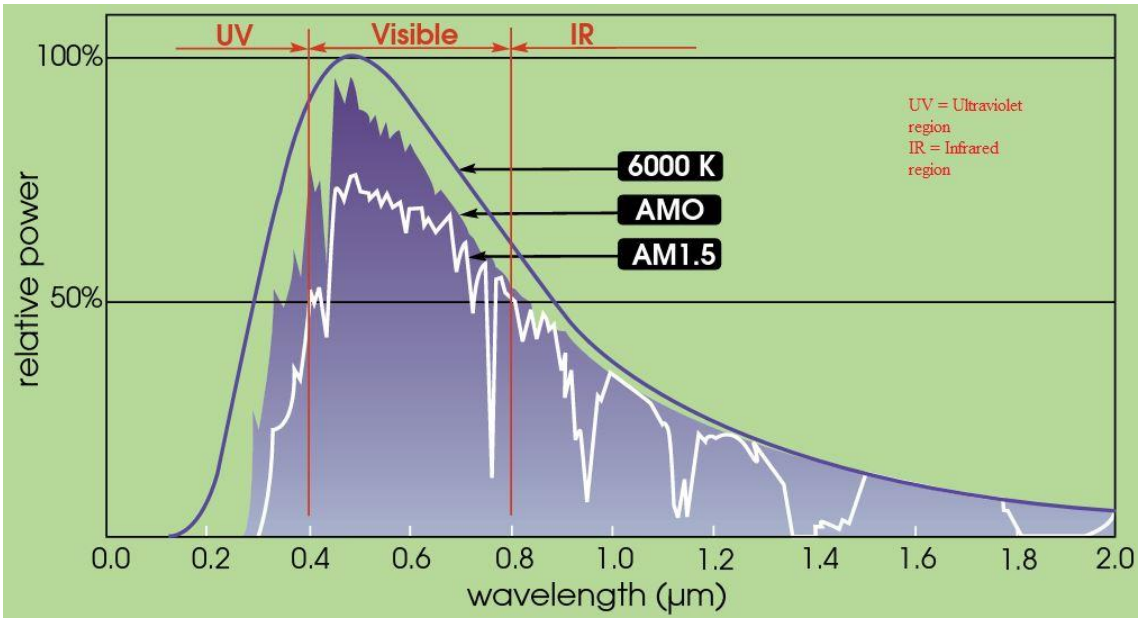

Figure 2.5 *Spectral distribution of solar radiation on the surface of earth [10]*

Air Mass (AM) is defined as the ratio of the path length of solar radiation to reach Earth's surface to the most shortest path. Air Mass zero (AM0) is the sunlight outside the atmosphere and Air Mass 1.5 (AM1.5) refer to the air mass or path length of sunlight coming through the atmosphere when the Sun is 48˚ from overhead. AM1.5 is used for the assessment of PV cells and power plants [10]. The loss in intensity of solar radiation due to the absorption and reflection by different particles in the atmosphere is measured by the air mass ratio [4]. The pictorial representation of the AM ratio is shown in figure 2.6.

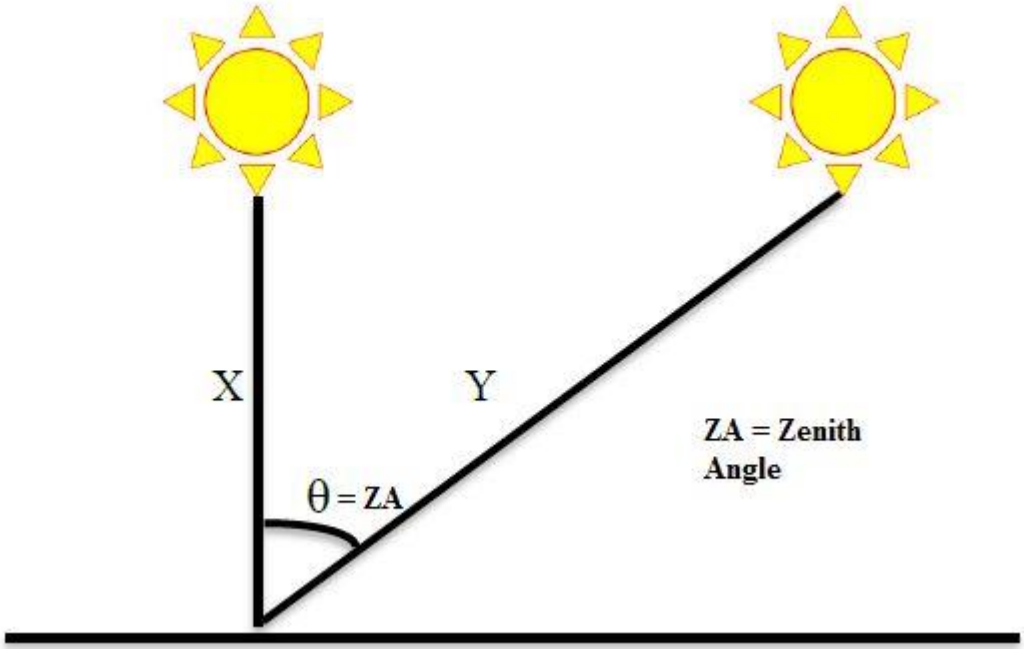

Figure 2.6 *Pictorial representation of AM ratio [4].*

The figure gives us the equation for the calculation of AM ratio which is as follows. An inverse cosine law determines the length of the path when the Sun is not overhead

$$AM = \frac{1}{\cos\theta}\,. \tag{2.8}$$

There are a lot of other factors which also need consideration when it comes to designing PV systems. The light which is absorbed by the solar cells is composed of three components which are the direct, albedo and diffuse components of solar irradiance. The light which comes directly without scattering in the atmosphere is the direct component. Some of the light is scattered by different dust particles and clouds in the atmosphere which makes up the diffuse component. Solar cells also absorb light which is reflected from the ground, trees, buildings and other surrounding land objects. This light makes up the albedo component. This component is quite significant in locations with heavy snowfall [11]. Figure 2.7 shows these different components

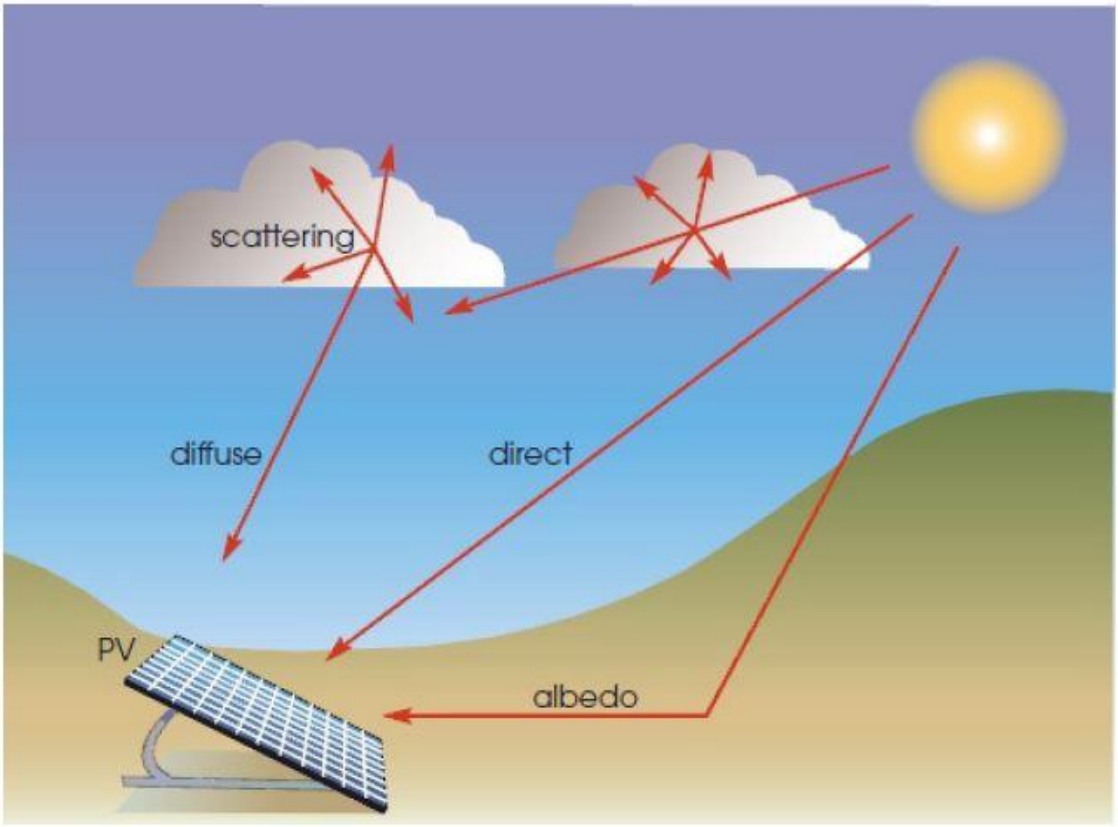

Figure 2.7 *Different components of sunlight [11].*

2.4 Photovoltaic cell

It is a well-known fact that at the heart of any photovoltaic power plant lies a solar module. This module is the main source of energy for the photovoltaic system. This solar

module is composed of solar cells which are either connected in series or in parallel depending on the desired operation [6]. Solar cells belong to the optoelectronic family of PN junction devices. They are also called photovoltaic cells. The energy conversion efficiency of photovoltaic cells varies between 15 to 30%. The physical features of a PV cell are identical to those of a PN junction diode with a slight variation in the shape of the electrodes which are finger shaped or transparent and allow light to strike the semiconductor [12]. The basic structure of a PV cell is shown in the figure 2.8

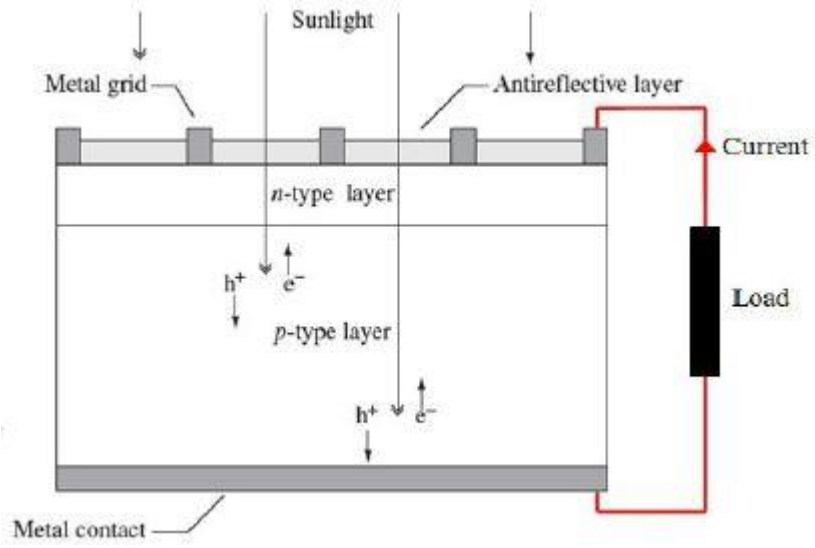

Figure 2.8 *Basic structure of a PV cell [13].*

Most of the PV cells are made up of semiconductor materials. This is the reason due to which semiconductor physics is applied to understand the fundamental operation of PV cells. Silicon is one of the most commonly used semiconductor material. It has four electrons in the valenced shell and is placed in the group IV of the periodic table of elements. Mature manufacturing technology, good light absorption properties and abundance in the Earth's crust make silicon the perfect candidate for manufacturing photovoltaic cells [14].

The main principle behind the energy band model is that the high energy bands are filled by the electrons from the low energy bands. Conduction band is the band having the highest energy. Energy gap (E_G) is the minimum energy required to move the electron from the valence band to the conduction band. It is given by the following equation.

$$E_G = E_C - E_V \,, \tag{2.9}$$

where, E_C is the minimum energy of the conduction band whereas the maximum energy of the valence band is E_V [14]. The energy bands of different materials are illustrated in the figure 2.9.

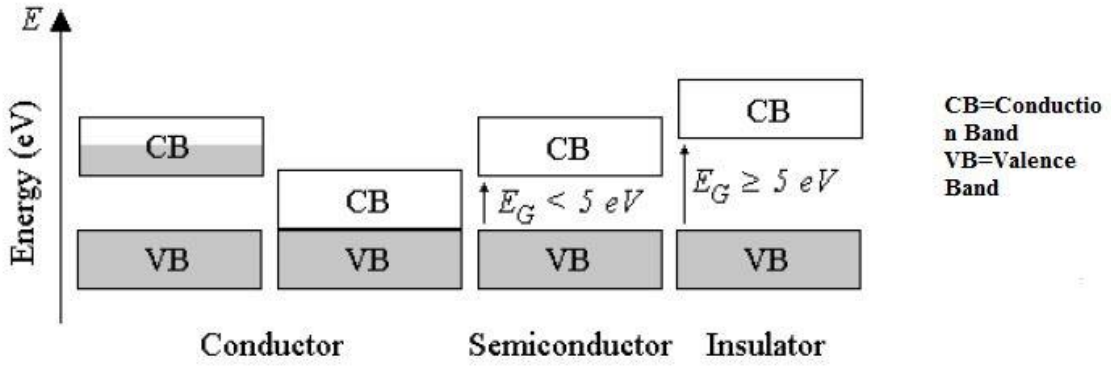

Figure 2.9 *Energy bands of different types of solids [14].*

Figure 2.9 shows that in semiconductors the conduction band and valence band are not overlapping but the bandgap energy is relatively small. This small bandgap energy can be overcome easily either by a DC voltage source or by an incident photon. Overcoming of this energy causes the electrons in the valence band to flow to the conduction band thus producing free current carriers. In photovoltaic cells these carriers are produced by the photons incident on the surface of the semiconductor device.

The light incident on the PV cell produces minority charge carriers. The built-in field diffuses the minority charge carriers through the junction and sweeps them across the junction. This causes a current flow out of the P terminal through the external short circuit and back into the N terminal. The current produced is called the short circuit current and is represented as I_{SC} [12]. It depends on operating conditions, cell structure and the properties of the material. Figure 2.10 shows this phenomena

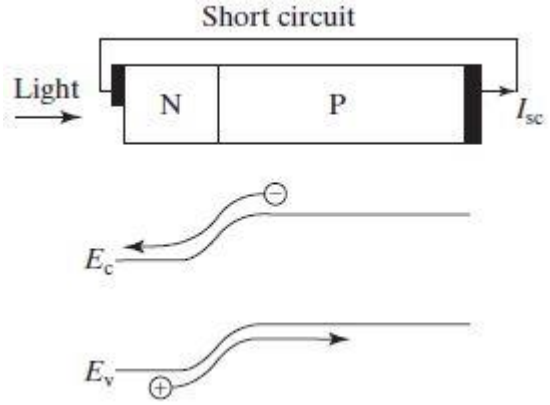

Figure 2.10 *Short circuit current [12].*

The total current generated by the PV cell is given in equation 2.10

$$I = I_{SC} - I_{01}\left(e^{qV/kT} - 1\right) - I_{o2}\left(e^{qV/2kT} - 1\right) \quad . \tag{2.10}$$

In the above equation I_{01} is the diode saturation current generated by the recombination in the quasi neutral region whereas I_{o2} is the saturation current due to recombination in the

depletion region, q is the electronic charge $1.6 \cdot 10^{-19}$ C, V is the voltage applied across the diode, k is the Boltzmann's constant $1.38 \cdot 10^{-23}$J/K and the T is the junction temperature in kelvins.

The magnitude of the voltage produced by a single PV cell of silicon is 0.6V. In order to obtain higher magnitude of voltage many cells of the same type are connected in series. A solar panel is formed by the parallel connection of several of these series connected PV cells and a significant number of solar panels together form a solar power plant also known as a photovoltaic system [12]. The MPP or the maximum power point is the point on the characteristic I-V curve of a solar cell at which the cell gives its maximum output power and to ensure operation at the MPP a load-matching circuit is used. The experimentally measured I-V curve of a silicon based PV cell is shown in figure 2.11.

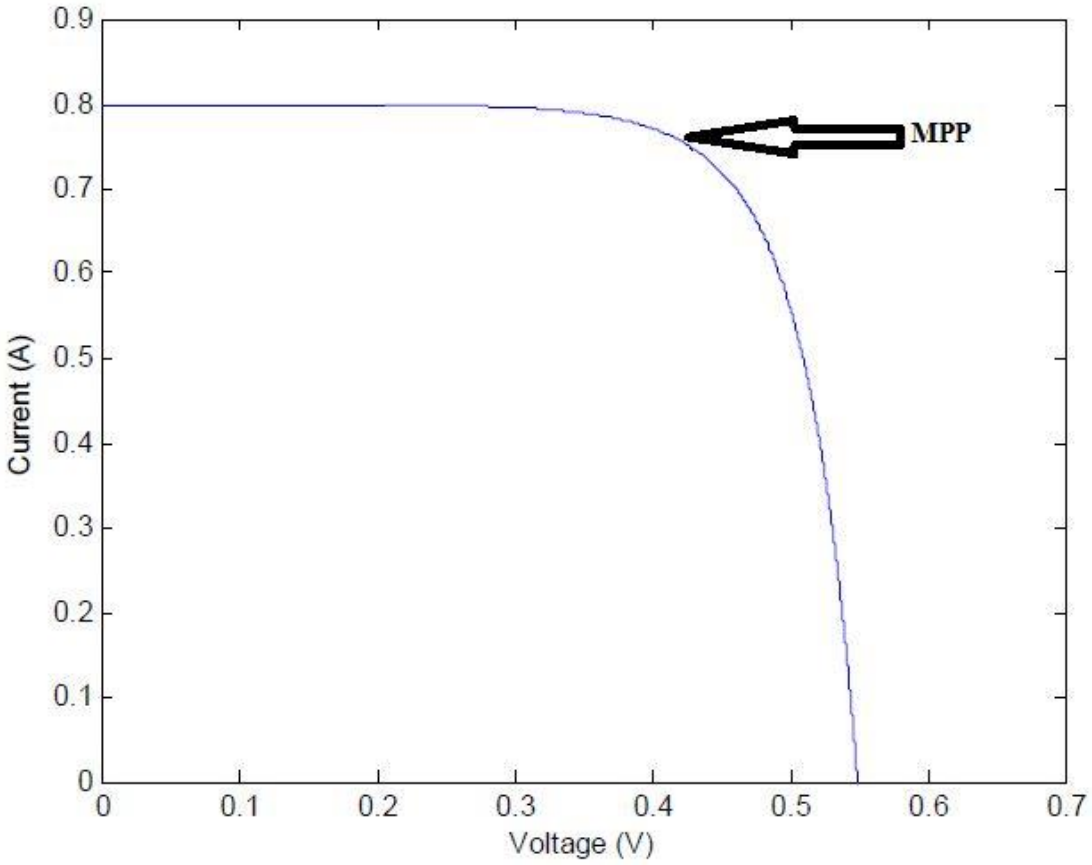

Figure 2.11 *I-V curve of a silicon based PV cell [14].*

The I-V curve in figure 2.11 is based on the following parameters. The short circuit current was 0.8 A and the temperature of the PV cell was 20˚ C. Solar cells also have the parasitic elements. They include the series resistance R_s and the shunt resistance R_{sh}. It has been found after careful experimentation that a small value of series resistance along with a higher value of shunt resistance gives the optimal performance of a photovoltaic cell [6].

2.5 Photovoltaic systems

Solar cells are rarely used as a single entity. This is because a single cell has a low operating voltage and high current with V_{oc} of 0.5 V. This voltage is much lower than the operating voltage of most of electrical loads and systems. The solution to this problem is the PV module. A PV module is composed of many cells connected in series. This raises the voltage to the desired level make it useful for daily applications. The most common example is the solar module with 36 silicon based solar cells connected in series used to charge 12 V batteries [10].

The connection of solar cells depends on the desired application. Cells are connected in series to increase the voltage level whereas they are connected in parallel for high current applications [15]. In the series connection the voltage of the solar module is the sum of the voltages of individual solar cells in the module whereas the same current flows through all of the cells. In the case of the solar cells connected in a parallel configuration the voltage across the terminals of a solar module is equal to the voltage of an individual cell in the module. However, the current is the sum of the individual cell currents [6]. The layout of a solar module with series connected cells is shown in the figure below

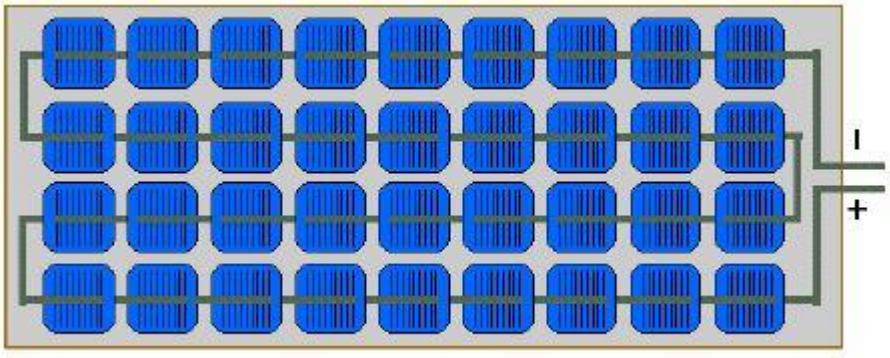

Figure 2.12 *Solar module with series connected cells [15].*

Shading of an individual cell degrades the performance of that particular cell thus resulting in mismatch. Series connection is more prone to mismatch when compared to the parallel connection [15]. The reason is that the shaded cell becomes reverse biased and acts as a load resulting in the heating of the PV cell and thus leading to cell failure. Bypass diodes are used to protect solar modules against this type of failure. The PV current flows through the bypass diodes if an individual cell is reverse biased as a result of shading [6]. Figure 2.15 shows the operation of a bypass diode when a PV cell is shaded

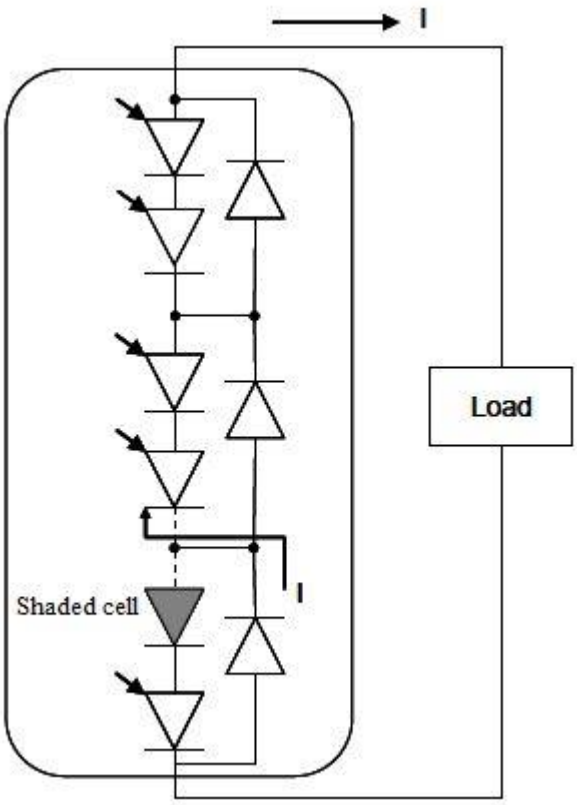

Figure 2.13 *PV module with bypass diodes [6].*

Photovoltaic systems are also connected to the grid and act as a source of distributed power. This connection of the PV power system to the grid has the advantage of effective utilization of power but the technical requirements of both the PV system side and the grid side need to be fulfilled. This ensures the safety of the utility grid along with that of the PV system installer. The inverter connects the PV power plant to the utility grid. Inverter is central to the grid connected PV systems as it converts the DC power from the solar modules to the AC power which is to be used by different electrical equipment and loads. The main technical issues involving the grid connected systems are islanding detection, electromagnetic interference and harmonic distortion requirements. These issues must be resolved before the connection of any PV system to the utility grid [16].

3. CLIMATIC PARAMETERS

3.1 Introduction

The operation of a photovoltaic power plant is affected by a number of environmental factors. They include the ambient temperature, global and diffused solar irradiance, wind speed and direction and humidity of the surrounding atmosphere. In this chapter the parameters which effect the operation of the PV power plant under real conditions will be discussed in detail. The different measuring techniques and instruments would also be explained.

The photovoltaic power plant at TUT uses an automatic weather station (AWS) to measure these environmental parameters. This weather station includes a network of measuring instruments that are spread over the power plant and are used to take the measure of the atmosphere surrounding the power plant. The various parameters include the global and diffuse solar radiation on the horizontal plane of the Earth, humidity, wind speed and direction and the ambient temperature [17]. The light sensing equipment used in the AWS is manufactured by Kipp & Zonen. The device used to measure the global solar radiation is the CMP22 pyranometer whereas the diffuse component of the solar radiation is measured using the combination of the CMP21 pyranometer with the CM121C shadow ring. The shadow ring blocks the direct component of radiation. The AWS also uses the sensors manufactured by Vaisala. These sensors include the WS425 ultrasonic wind sensor used to measure the speed and direction of the wind. Moreover, the ambient temperature and humidity of the atmosphere is measured using the HMP155 sensor.

The location of the sensors in the PV power plant is of great importance to the accuracy of the measurements. The global solar radiation sensor CMP22 and the ultrasonic wind sensor WS425 should be placed in a location where there is no disturbance due to the surrounding structures. This is the reason both these sensors have been installed at the highest point of the rooftop. The temperature and humidity sensor along with the sensor which measures the diffused solar radiation is installed on the lower rooftop. This is because the CM121C shadow ring needs to be adjusted and is easily accessible when installed on the lower rooftop [17].

The module temperature and irradiance is also measured and closely monitored. The temperature sensor used is Pt100 and SPlite2 sensor is used to measure the irradiance received by the modules [18]. These sensors are also manufactured by Kipp & Zonen and are the state of the art measuring instruments. Both these sensors are used in pairs providing accurate information on the operating condition at module or string level. Pt100 temperature sensors are located on the back plates of the solar modules whereas SPlite2 sensors have been installed in a tilted position with the same angle as the solar modules [17]. The

analysis of the data has been made possible due to the continuous recording and storage in the database. Figure 3.1 shows the module irradiance and temperature sensors

(a) *(b)*

Figure 3.1 *(a) SPlite2 irradiance sensor (b) Pt100 temperature sensor.*

3.2 Global radiation

Global solar radiation includes radiation received directly from the solid angle of the sun's disc. Radiation on the Earth's surface plays a vital role in the heat economy of our planet. Global solar radiation also includes the diffuse component of light which is formed as a result of the scattering of light due to the presence of micro particles in the atmosphere [19].

The instrument which is used to measure the global solar radiation is the pyranometer. It is also used to measure the reflected global radiation but in this case it has an inverted orientation. The continuous exposure of pyranometers to outdoor environments makes it a necessary requirement that they are highly durable and should operate effectively in all weather conditions. Global radiation on horizontally inclined surfaces is also measured using the pyranometer. The spectral range of a conventionally standard pyranometer is between 300 nm to 3000 nm and it measures global radiation in watts per square meter (W/m^2) [19]. This is shown in the figure 3.2.

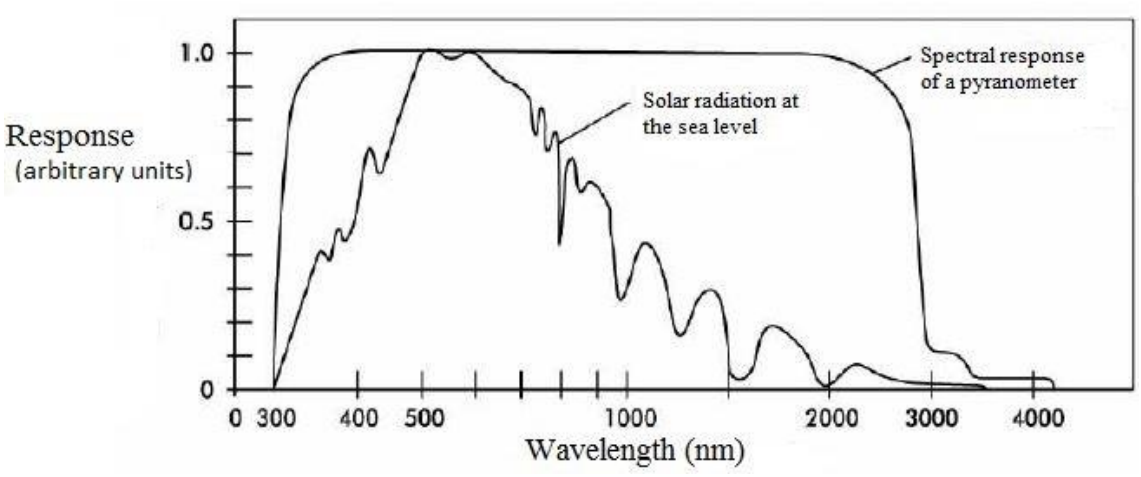

Figure 3.2 *Standard pyranometer spectral response [6].*

The solar photovoltaic power plant at TUT uses the Kipp & Zonen CMP22 pyranometer for measuring global solar radiation. It is a state of the art instrument for measuring global solar irradiance incident on it from the hemisphere above it. Glass domes and thermopile detectors are used to meet the directional and spectral requirements in these pyranometers. A small voltage is generated when radiation falls on the light sensing element of the pyranometer. This is the voltage on which the pyranometer operates hence making it independent of external power supply. The requirements of the ISO 9060:1990 standards are fulfilled significantly by the CMP22 pyranometer along with the compliance with IEC 60904-1 [20]. Compliance with the international standards ensures that the CMP22 can be operated in any kind of environment without affecting its performance. Figure 3.3 (a) and (b) illustrate the CMP22 sensor.

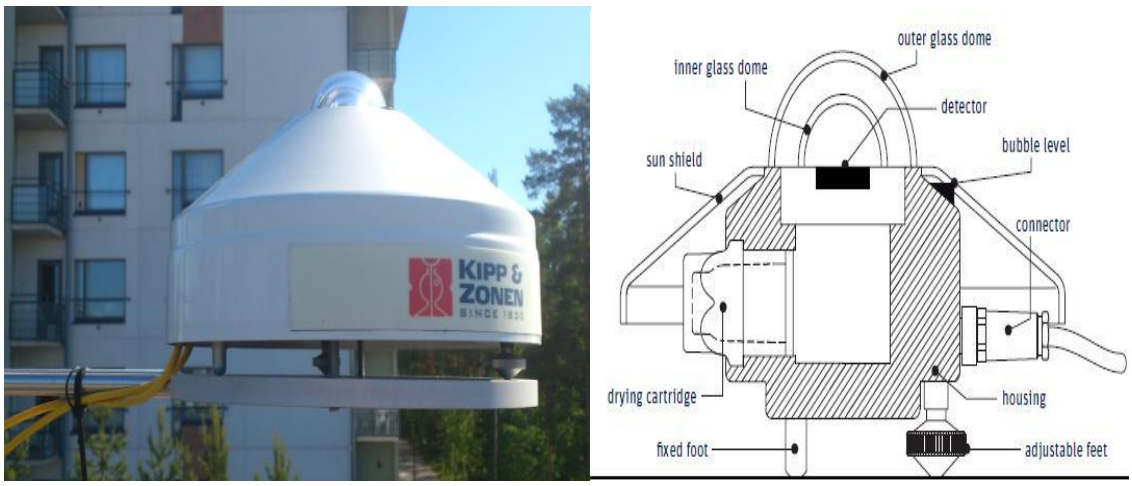

Figure 3.3 *(a) Installed CMP22 pyranometer (b) Structure of a CMP22 [20]*

Global solar irradiance can be calculated by dividing the output voltage of the sensor by its sensitivity value. Calibration of this pyranometer is done after two years of operation with a factor of 9.52 $\mu Vm^2/W$ [11].

3.3 Diffused radiation

In order to measure the diffuse component of solar radiation precisely the photovoltaic power plant at TUT uses the CMP21 pyranometer with the CM121C shadow ring. Both of these instruments are designed and manufactured by KIPP & ZONEN who also specify the alignment procedure for the shadow ring. The shadow ring installed at the power plant along with the CMP21 pyranometer is shown in figure 3.4

Figure 3.4 *CMP21 pyranometer with CM121C shadow ring.*

The shadow ring should completely cover the dome of the pyranometer. This requires the shadow ring to be regularly adjusted as there are changes in the solar course on a daily basis. It should also be noted that the ring also blocks some of the diffuse radiation from reaching the pyranometer which means corrections should be made to the measurements. The calibration factor for the CMP21 pyranometer is 8.89 $\mu Vm^2/W$ [11].

The alignment of the shadow ring involves three steps. Firstly, the shadow ring should be aligned to the axis of north to south. It is better that this alignment procedure is done at 12.00 true solar time. True solar time can be obtained from an astronomic observatory facility. Depending on the location at this particular time the Sun is either shining from the north or the south [21]. Alignment procedure also involves the setting of the shadow ring sliding bars and tilting of the sliding bars. Shadow ring sliding bars need to be adjusted from time to time for accurate measurements. The adjustment should be done according to the tables provided in the user manual which can be accessed directly from the link provided in [21]. The inner side of the ring should not be exposed to the sunlight.

Both the CMP21 and CMP22 are robust instruments with a capability of operating effectively in the sub-zero temperatures of Finland. The temperature range of both these instruments is -40˚- +80˚ C. The difference between the two devices is the presence of top quality quartz domes in CMP22 which minimize the directional error [20].

3.4 Temperature

Temperature measurements are very sensitive to undesired disturbances. The best solution to eliminate these disturbances is the application of a radiation shield. The thermometer should be completely encapsulated inside the shield so that it is protected from radiant heat, rain and any other phenomena that might affect the measurement. The height of the temperature sensor should be 1.2-2 m from the ground level [6]. The instrument used to measure the temperature at the TUT solar PV power plant is the HUMICAP humidity and temperature probe HMP155 manufactured by VAISALA. Resistive platinum sensors (Pt100) are used to measure the temperature. In harsh environments such as fog, mist and rain the sensor probe is supplied constantly with heat so that is does not get condensed because condensation reduces the life span of the sensor. The different voltage ranges measured by this sensor are between 0-1 V, 0-5V and 0-10V. The installed HMP155 sensor along with the DTR503A and DTR502A radiation shields can be seen in the figure 3.5 [22]

Figure 3.5 *HMP155 sensor with the DTR503A and DTR502A radiation shields installed at TUT PV power plant.*

The sensor can measure a temperature between -80 - +60 ˚C which makes it suitable to operate in Finland where the temperature fluctuates typically between -30 - +30 ˚C. The instrument is designed in a way that the sensor is located on the tip of the temperature

probe and is protected by a removable filter. This makes the sensor to operate accurately in all kinds of harsh environments [22].

3.5 Humidity

The measurement of atmospheric humidity is central to the effective operation of PV power plants. Humidity is defined as the partial pressure of water in the atmosphere [19]. Relative humidity is the ratio of the observed vapour pressure to the saturation vapour pressure with respect to water at same temperature and pressure. It is measured in per cents. Humidity can also be related to the changes in the state of the water in the air. This makes the measurement of humidity very central to meteorological analysis and forecasting [6]. The instrument used to measure the humidity is called the hygrometer. It measures the dew-point temperature and relative humidity. There are different methods to measure the humidity which include the sorption method, condensation method, psychrometric method and the gravimetric hygrometry [19].

HMP155 temperature and humidity probe is used to measure the humidity at the TUT PV power plant. The capacitive thin film HUMICAP180RC polymer sensor measures the humidity [22]. The protection of the sensor against water, dust and dirt is achieved by the sintered Teflon filter. In rapidly changing temperatures the device is able to take accurate measurements because of the fast response time of the sensor [11]. The sensor along with the temperature probe is shown in figure 3.6. The figure illustrates the different parts of the sensor including the filter, protection cover and the 8-pin male connector M12. In places where there is constant high humidity the temperature of the humidity probe increases for better performance. The humidity is measured between 0-100%.

Figure 3.6 *HMP155 sensor with structure of the probe (1) Filter (2) Protection cover (3) 8-pin male connector M12 [22].*

3.6 Wind speed and direction

Wind speed is a 3D vector quantity which fluctuates on a small scale in space and time superimposed upon a large scale organized flow however for the purpose of this thesis wind will be taken as a 2D quantity with speed and direction. The 3D nature of wind is considered only when it is measured with reference to airborne pollution and landing of an aircraft. The level of rapid fluctuations in the wind by which it is characterized is called gustiness with the single fluctuations known as gusts [19]. The main factor behind the winds is the difference in heating of the equator and the poles which is due to a difference between the levels of absorbed solar energy and also the rotation of the Earth.

Anemometers are used to measure the speed with which the wind is blowing. This instrument should be placed at a considerable height at which it is sufficiently exposed to the wind and the path of the wind should be clear from any kind of physical barriers and obstructions. The direction of the wind is either measured by a windsock or by a banner mounted on a pole with the principal points of the compass [19]. But when it comes to measuring wind for research purposes ultrasound signals are used because they allow us to take the measurements with a high frequency. The measurement of wind speed is very important to the operation of PV power plants because the module temperature is significantly affected by the wind due to the convection coefficient. Nowadays sonic anemometers, cup and propeller sensors and direction vanes are the instruments which measure the properties of the wind. These instruments are state of the art technology for the digital measurement of wind [6].

The instrument which is used to measure the properties of the wind at the TUT solar PV power plant is the VAISALA WINDCAP ultrasonic wind sensor WS425. It includes an onboard microcontroller which records and processes the data and also performs serial communication. The structure of the sensor is composed of three ultrasonic transducers mounted on a horizontal plane with equal spacing. The time taken by the ultrasound to travel from one transducer to the other transducer is measured in both directions and this time is dependent on wind speed. The following equation is used to calculate the speed of the wind

$$V_W = 0.5L\left({}^{1}/_{t_f} - {}^{1}/_{t_r}\right). \tag{3.1}$$

In this equation V_W is the velocity of the wind, L is the distance between the two transducers, t_f is the transit time in forward direction whereas t_r is the transit time in reverse direction. The calculated wind speed does not depend on the humidity, temperature and altitude. The transit times are only affected by the velocity of sound [23]. The installed WS425 sensor can be seen in the figure 3.7

Figure 3.7 *WS425 ultrasonic wind sensor.*

This sensor does not require any type of maintenance and the mean time between the failures is 26 years in theory. The transducers are not affected by rain and the sensors are made of stainless steel which is the reason the sensor can operate efficiently in any kind of environment. The sensor should be placed at a high point within 300m of horizontal radius with a lightning rod to protect it from lightning surges [11]. The tip of the lightning rod should be one meter in height.

The parameters of the wind such as speed and direction are measured as voltages by this instrument. Wind speed is 0 m/s when the voltage is 0 V whereas it is 55.88 m/s when the voltage is 1 V. Voltage range in order to measure the wind direction is 0-4 V. In this case 0˚ is represented as 0 V whereas 360˚ is represented by 4 V [4].

4. TUT SOLAR PV POWER RESEARCH PLANT

4.1 Introduction

This chapter gives an introduction of the PV power plant installed at the rooftop of the Department of Electrical Engineering at TUT. The plant was finalized during the spring of 2010. The plant has an automatic weather station which takes a measure of the environmental parameters which affect the PV modules along with a mesh of module temperature and irradiance sensors attached to the individual PV strings. This chapter will explain the layout and configuration scheme of this power plant which will give us an insight on the real time operation of the power plant.

The state of the art data acquisition system which enables the real time data to be available on the department's website is also briefly explained. The recording of data at all times gives the capability to study the daily, seasonal and annual profiles for diffused and global radiation, wind speed and direction and temperature and humidity. It also enables us to study module temperature. These type of studies are a cornerstone for this master's thesis as they provide a solid ground to study the correlation between various quantities which directly or indirectly affect PV power.

The main objective of this power plant is its application for research purposes which involves the effect of different types of connection of PV strings on the power production, testing and evaluation of power electronics equipment and to study the effect of environment on the performance of the power plant and individual PV strings. It is important here to mention the name of Mr. Diego Torres Lobera who finalized the selection of all the hardware and software equipment for the plant and published it in his master's thesis in 2010 [6].

4.2 Plant layout and configuration

The power plant installed at TUT is a grid connected system. It has an installed capacity of 13.1 kW (kilowatts) generated by 69 NAPS NP190GK photovoltaic modules [24]. An individual PV module is composed of 54 series connected polycrystalline silicon cells. There are two possibilities for the configuration of this power plant. One is the 4-output configuration with three strings of 17 PV modules and a single string of 18 PV modules. The 3-output configuration is composed of three strings of 23 modules each. The modules are divided into 6 strings and are installed in a way to minimize the effect of shading cause due to shadows on the PV modules. The electrical characteristics of an individual PV module are shown in the table 1. These involve the power at the MPP, voltage at the MPP, current at the MPP, short circuit current, open circuit voltage, weight and dimensions.

Table 1 *Characteristics of a NAPS190GKg PV module under standard test conditions [24]*

Quantity	Value
Power at MPP P_{MPP}	190 W
Current at MPP I_{MPP}	7.33 A
Open Circuit Voltage V_{OC}	33.1 V
Short Circuit Current I_{SC}	8.02 A
Voltage at MPP V_{MPP}	25.9 V
Weight	19.5 kg
Dimensions (length, width and thickness)	1475mm x 986mm x 35mm

The 3-output configuration has a maximum power of 4.2 kW with voltage at the MPP at 596 V and an open circuit voltage of 761 V. The three 17 panel strings in the 4-output configuration have a P_{MPP} of 3.1 kW with V_{MPP} at 440 V and V_{OC} at 563 V. The single 18 panel string has a power of 3.3 kW at the maximum power point with a voltage of 466 V at the MPP and an open circuit voltage of 596 V [6]. The pictorial depiction of the TUT solar PV power plant can be seen in the figure 4.1

Figure 4.1 *Solar PV power facility at TUT [24].*

4.3 Measured data acquisition system

Data acquisition systems are central to the optimum performance of renewable energy systems used for research purposes such as the PV power plant at TUT. These systems record the valuable data which plays a vital role in the feasibility studies of renewable energy systems. The technology for data acquisition systems is mature and many such systems are available to measure the performance of PV power plants in real operating conditions [25]. The data acquisition system at the TUT solar PV power plant is manufactured by National Instruments (NI) and uses the LABVIEW program. This system is computer based and can be seen in the figure 4.2

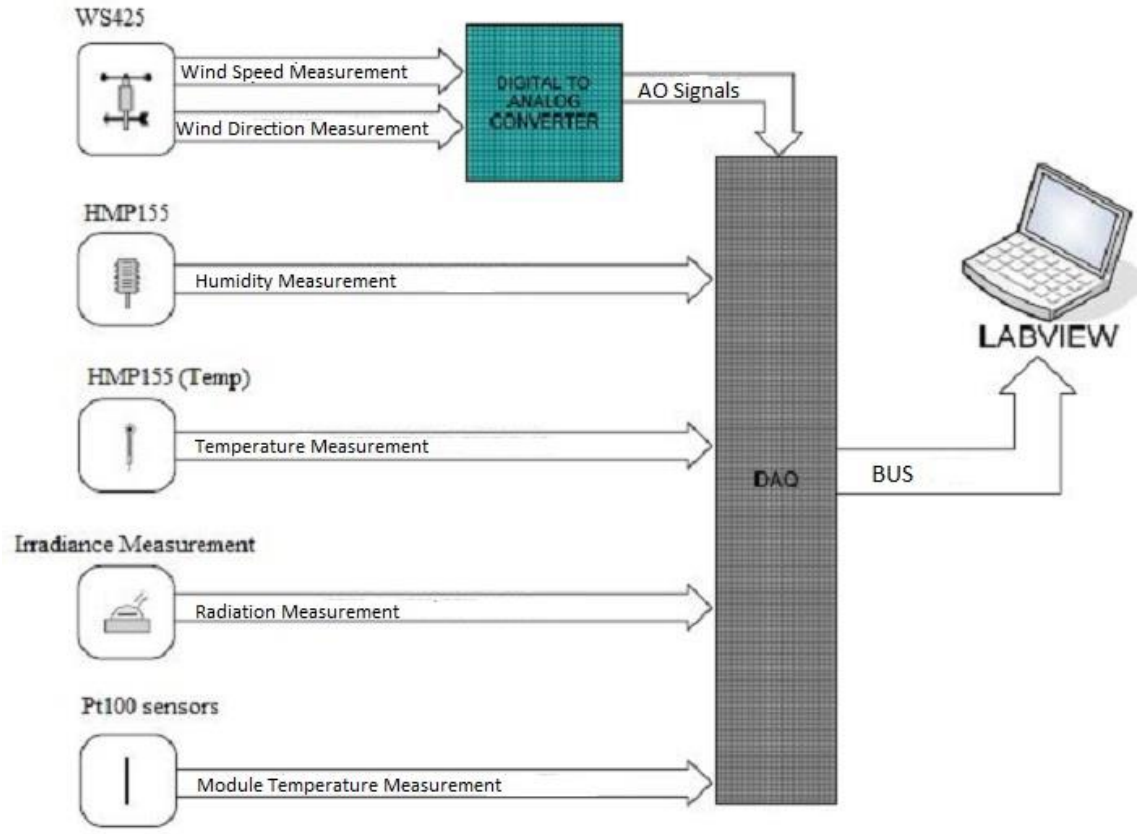

Figure 4.2 *Measured data acquisition system [6].*

The hardware components of this system include the compact RIO-9074 controller, NI 9144 chassis, two NI 9205 modules, six NI 9217 modules, back-UPS RS800 and the host computer [11]. In order to transmit and receive the signals provided by the measuring equipment a master and slave system is used in which the RIO units are receiving and the data is being continuously sent to the master unit by the slave. This data is then acquired by the PC from the master by the utilization of an Ethernet cable. One advantage of this system is that it reduces the length of the Ethernet cables by locating the units to the closest possible sensors. The other benefit of this system is that it can be easily extended in the future by either replacing or adding more I/O modules.

5. MEASURED DATA ANALYSIS

In this chapter the behavior of the various environmental parameters is shown and analyzed. The variations in the profiles of these parameters is studied both annually and seasonally. The basic aim of this chapter is to compare these profiles. This comparison will help to find a correlation between these parameters which can then be used to optimize the operation of solar PV power plants particularly the solar PV power plant at TUT. The data for the summer season includes the data from the months of May, June and August and for the autumn time it involves the months of September and October if not mentioned otherwise. The winter data has been taken for the months of November to February and for spring the data has been recorded for the months of March and April if not mentioned otherwise. The time between successive measurements is one second and the average values are recorded for four hours between 10:00-14:00 hours for solar radiation and wind speed if not mentioned otherwise. The averages have been calculated using the Microsoft Excel computer software.

5.1 Global solar radiation

The sun emits constant energy during the course of the year but the irradiance received on the Earth surface varies all the year around. There are many reasons for this variation which includes the position of the sun, scattering in the atmosphere and the variations in atmospheric conditions. Figure 5.1 shows the annual profile of the average daily global solar radiation received at the TUT solar PV power plant. The measurements have been taken for the year 2014 by the CMP 22 pyranometer. The average daily global solar radiation values for the month of July 2014 are missing because of undesired interruption in the data recording. The time interval between two successive readings was 1 second so that the smallest possible variation can be detected.

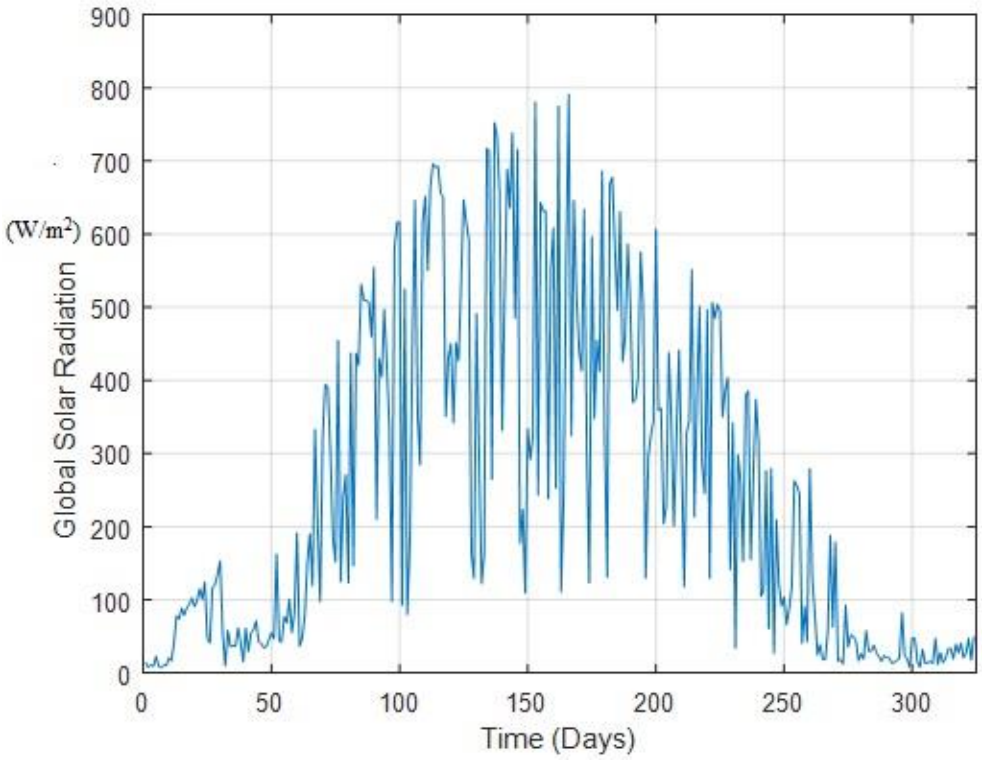

Figure 5.1 *Average daily global solar radiation profile at the TUT PV power plant for the year 2014.*

The figure 5.1 illustrates that the highest amount of average daily global solar radiation is received during the summer time particularly during the months of June and August. The highest average daily value of global solar radiation recorded during these months was 791.1 W/m^2. The reason for such high value is the longer duration of sunlight, large amount of clear sky days and less humidity. It can be seen from the daily global solar radiation profile that the solar irradiance starts declining during the autumn time in the months of September and October and reaches its minimum value in the winter months of November, December, January and February. The main reason for the low amount of irradiance is lack of sunlight, heavy cloud cover, humidity and snow depth. The lowest recorded average value of daily global solar radiation was 6.935 W/m^2 received during the month of January 2014. The seasonal behavior of the daily global solar radiation was also recorded and studied. Figure 5.2 shows the seasonal behavior of the average daily global solar radiation

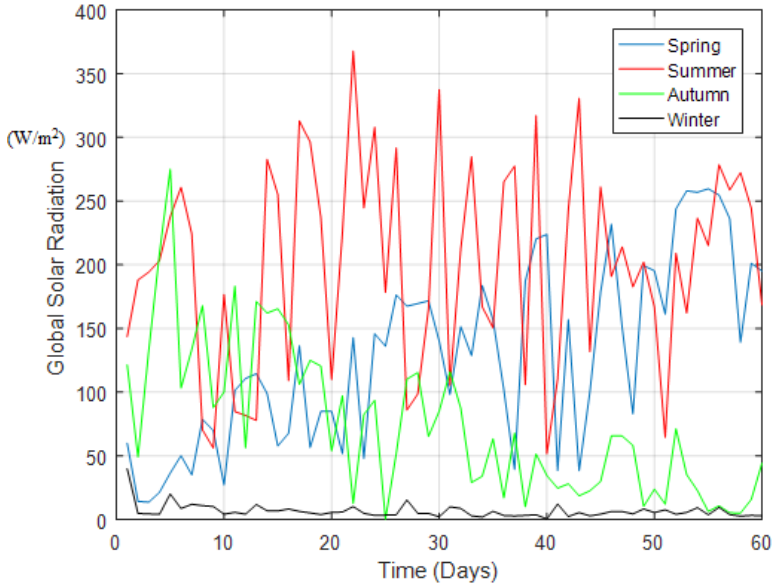

Figure 5.2 *Seasonal behavior of average daily global solar radiation at TUT solar PV power plant for 2014.*

In this case the measurements were taken for the whole course of the day and the time interval between successive measurements was 1 second. The figure 5.2 shows the daily average values of global solar radiation. It can be seen clearly that the lowest amount of average daily global solar radiation is received during the winter time. The maximum value of which is 39.95 W/m^2. The values follow an increasing trend during the spring time and reach their maximum in the summer time. During the autumn season the average daily global solar radiation follows a decreasing trend due to the gradual reduction of the daylight hours and the increased amount of cloud cover. The same happens but in reverse in the spring time.

5.2 Diffused solar radiation

In order to study the irradiance received by a PV power plant in detail it is therefore fundamental to study also the diffused component of solar irradiance. Diffused solar radiation is caused by the scattering of light in the atmosphere and also due to the collision of light with the objects surrounding the PV power plant. Figure 5.3 shows the average annual diffused solar radiation profile of the TUT PV power plant for the year 2014. Some of the data is missing due to the undesired interruption in the data recording.

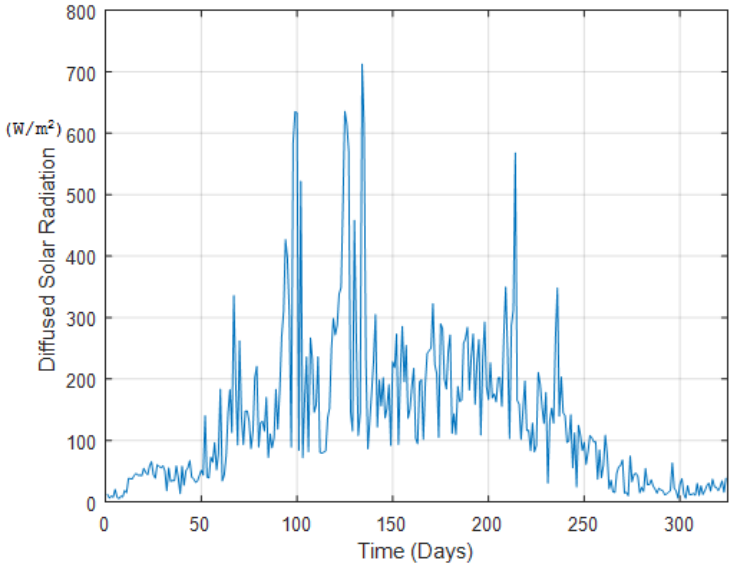

Figure 5.3 *Average daily diffused solar radiation profile at TUT for 2014.*

Diffused solar radiation follows an increasing trend from mid-March till mid-May but after that there is no sharp rise in diffused solar radiation in the summer months. The main reason for this behavior is the increased number of clear sunny days during the summer time. We can see that there is a sharp increase in the diffused solar radiation for some days during the spring and autumn time. This may be caused by the disoriented position of the shadow ring leading to a measurement error. Generally, during the autumn time diffused solar radiation decreases due to the onset of the winter. This same trend can also be seen in the seasonal behavior of the diffused solar radiation as shown below in figure 5.4. In this case the average values are for the whole course of the day with the same measurement settings as used for the annual diffused solar radiation profile. The sharp rise in diffused solar radiation here is also due to the measurement error.

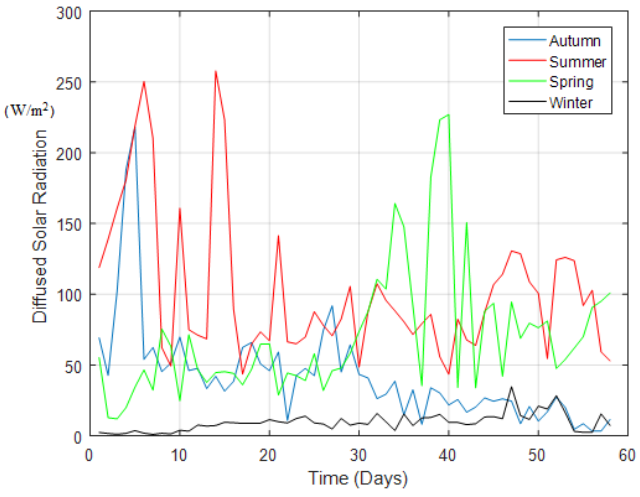

Figure 5.4 *Diffused solar radiation average daily seasonal profile at TUT solar PV power plant for 2014.*

The most important thing is to study the annual and seasonal comparison of global solar radiation with diffused solar radiation particularly during the winter season. This is done in order to visualize the contribution of diffused solar radiation to global solar radiation over the course of a year and different seasons. The comparison of global solar radiation with diffused solar radiation for 2014 can be seen in figure 5.5.

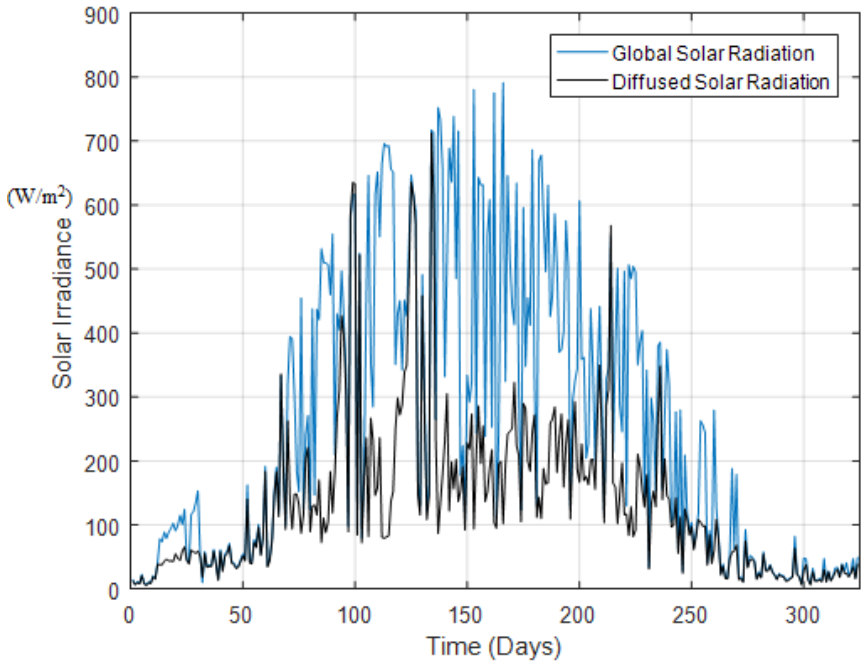

Figure 5.5 *Average daily solar irradiance at TUT PV power plant for 2014.*

It can be seen clearly that during the winter the solar irradiance is entirely composed of diffused solar radiation and the amount of global solar radiation is negligible. The reason for this decline is heavy cloud cover, humidity and the lack of sunlight due to the short span of daytime in the winter. This can also be confirmed from the seasonal behavior of solar irradiance. In this case data has been recorded for the winter months of November, December, January and February 2014. This can be seen in the figure 5.6 below. It shows that for most of the days during the winter time the global and diffused solar radiation are same. The amount of solar irradiance is very low with a maximum value of 39.85 W/m^2. It is therefore important to harvest each and every amount of solar radiation during the winter time for the efficient running of PV power plants.

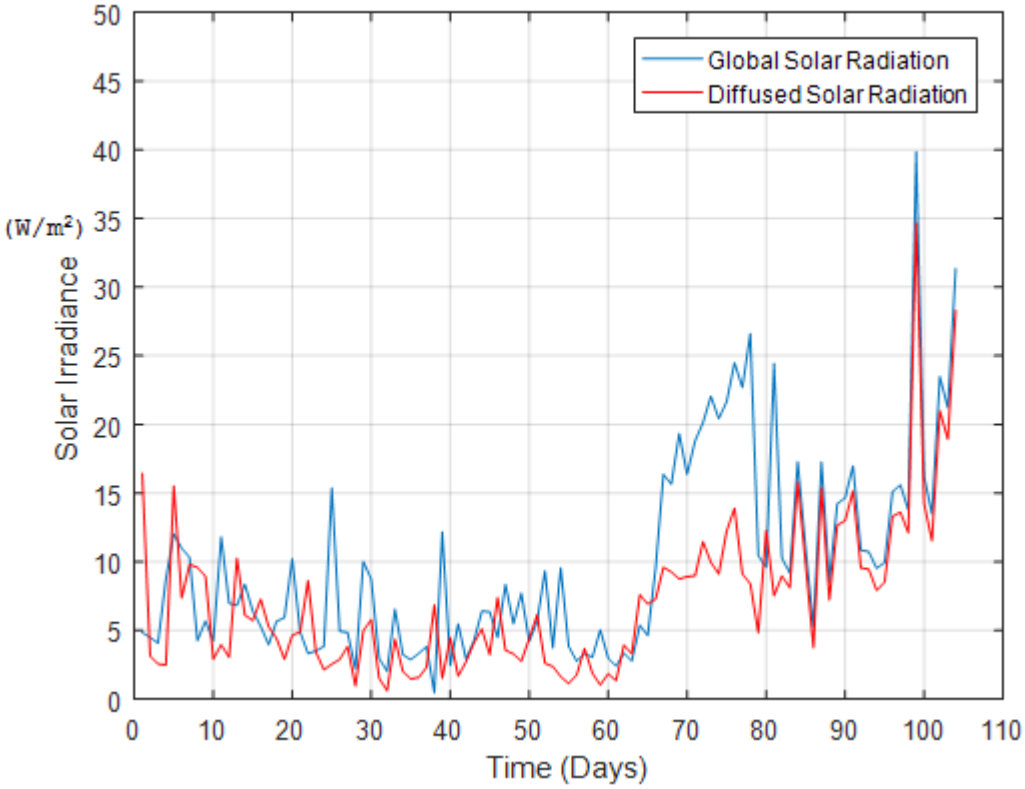

Figure 5.6 *Average daily Solar irradiance at TUT PV power plant for winter 2014.*

5.3 Ambient temperature and humidity

In this section the annual and seasonal profiles for the ambient temperature and the atmospheric humidity at the TUT PV power plant would be studied. The measurements have been taken using the HMP155 temperature and humidity probe for the whole course of the year 2014. The single average daily value has been calculated from measurements for the whole 24-hour course of the day using the Microsoft Excel computer software. Figure 5.7 shows the daily behavior of the average ambient temperature. Some of the data is missing due to undesired interruption in data recording.

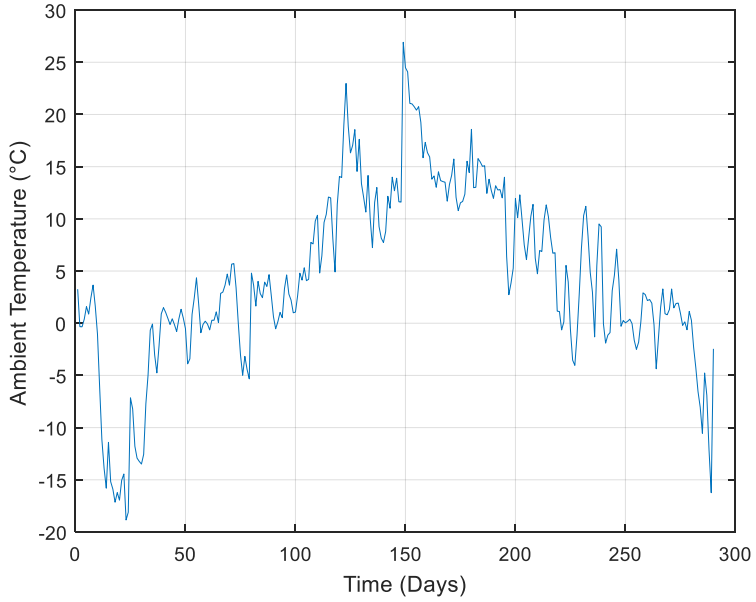

Figure 5.7 *Average daily ambient temperature profile at TUT PV power plant for 2014.*

The average temperature drops to a minimum of -18.85 °C during the start of the year. This is particularly due to the cold winter months of January and February when there is snow cover in Finland. The annual profile of ambient temperature illustrates that from mid-March to August there is an increasing trend in the average temperature and it reaches its maximum value of 26.91 °C in the summer. This trend is due to the hot summer months of June and August, longer duration of sunlight and clear skies and lower humidity. During the autumn time the temperature slowly and gradually starts decreasing reaching its minimum during the winter months. This behavior can be more clearly seen in the seasonal behavior of ambient temperature as shown below in figure 5.8

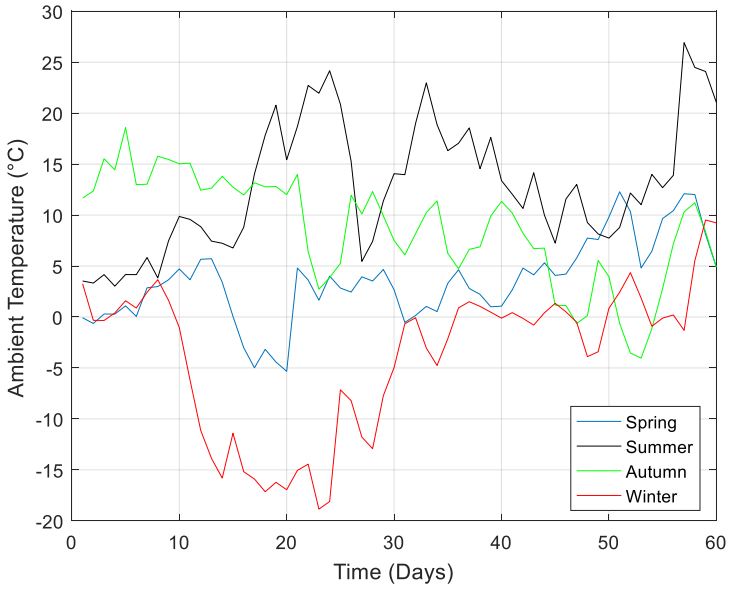

Figure 5.8 *Seasonal behavior of average daily ambient temperature at TUT PV power plant for 2014.*

Humidity of the atmosphere also plays a vital role in the operation of PV power plants. Previously conducted studies conclude that the increase in amount of humidity in the atmosphere increases the amount of diffused solar radiation thus leading to a low efficiency of the PV power plant [4]. It is therefore very important to study the behavior of humidity over the course of a year and in different seasons. This behavior can then be used for comparison with other environmental parameters such as ambient temperature. Figure 5.9 shows the annual profile for the humidity at TUT PV power plant for the year 2014

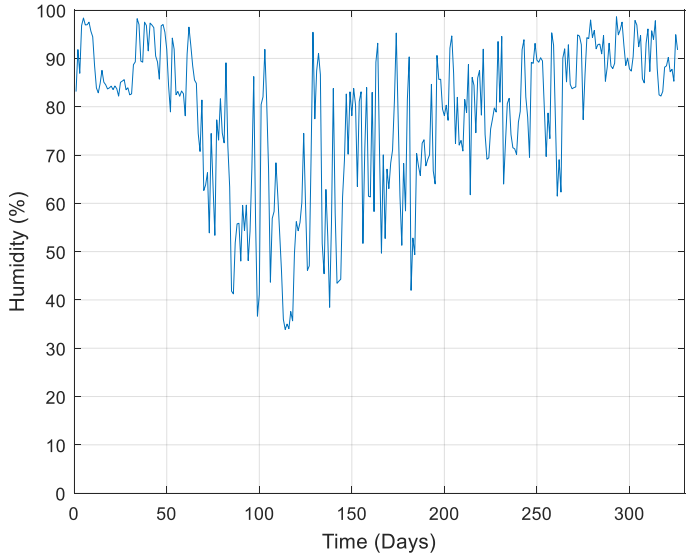

Figure 5.9 *Average daily humidity profile for 2014 at TUT PV power plant.*

It can be seen from the figure 5.9 that there is a decreasing trend in the humidity of the atmosphere from spring onwards till the summer time with a minimum value of 33.87%. It should also be noticed that there is a lot of variation in the humidity in the summer months with values oscillating between 38-95%. The reason for these variations is the continuous change between the clear sky and cloudy days during the summer with low humidity in clear sky conditions. This variation in the atmospheric humidity decreases with the arrival of the autumn and is almost negligible during the winter time when it oscillates between 82-97%. We can conclude from the humidity profile that the atmospheric conditions vary a lot during the summer time as compared to the winter time when there is almost constant cloud cover. This can be further confirmed by the individual profiles of humidity for winter and summer as shown in figure 5.10

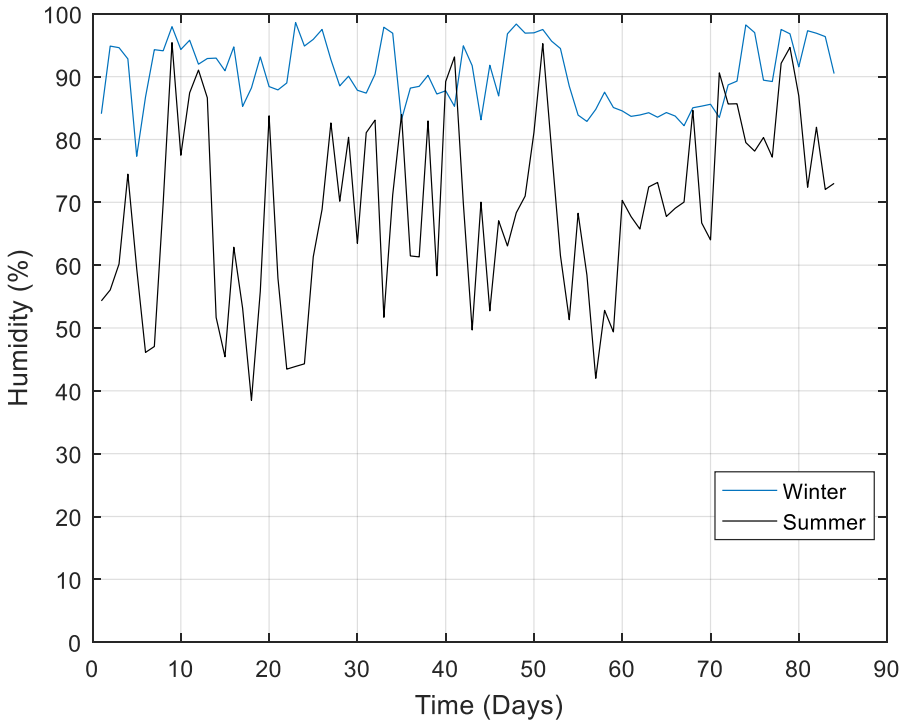

Figure 5.10 *Average daily winter humidity and average daily summer humidity at TUT PV power plant for 2014.*

The comparison of ambient temperature with humidity was also analyzed. In this case, average monthly values for 2014 were calculated and plotted using MATLAB. It can be seen in figure 5.11 below. The figure illustrates that for most of the time when the ambient temperature is increasing the humidity follows a decreasing trend. During the summer time due to clear sky conditions and longer sunlight hours the humidity is very low and subsequently there is an increase in the ambient temperature. The case is completely opposite in the months of winter when heavy cloud cover and shorter duration of daylight hours causes a sharp decrease in the ambient temperature. However, there are some exceptions to this relationship due to the presence of some cloudy days during the summer and some clear sunny days during the winter season.

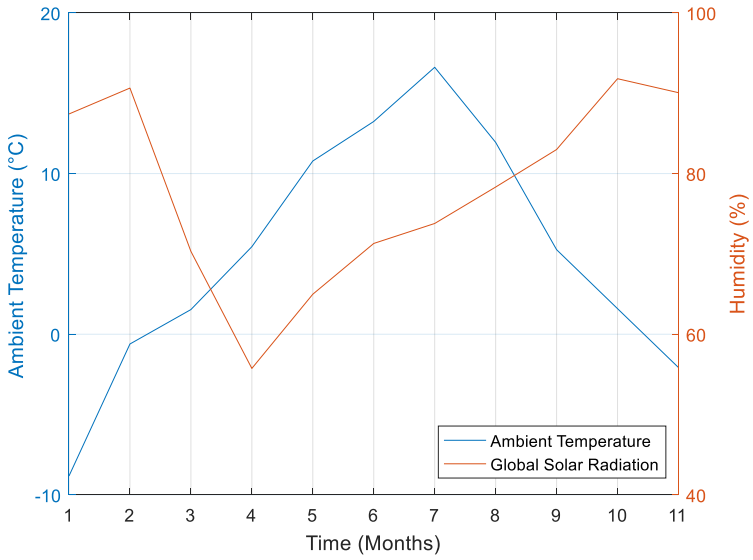

Figure 5.11 *Monthly average ambient temperature and monthly average humidity for 2014*

The above relationship between ambient temperature and humidity makes it easier to understand the relationship between global solar radiation and humidity. The monthly average values of both these parameters were compared for the year 2014 with the same measurement settings as in figure 5.11. It was found that with an increase in global solar radiation the humidity subsequently decreases and vice versa. This can be seen in figure 5.12 below

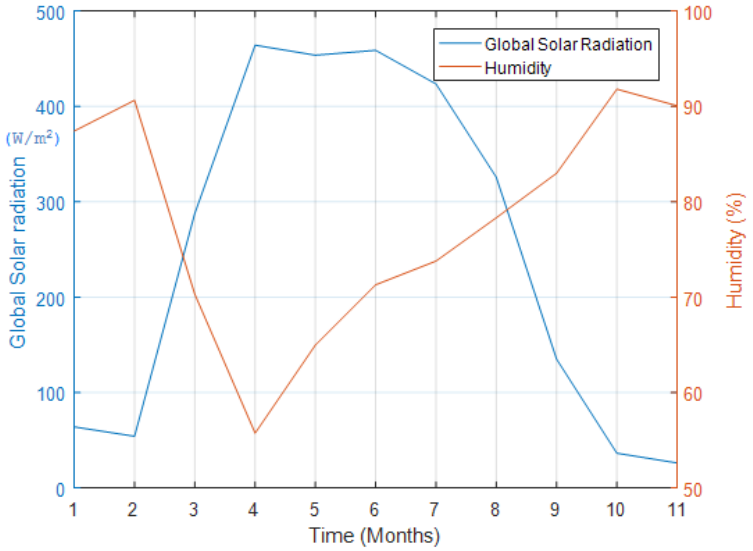

Figure 5.12 *Monthly average global solar radiation and monthly average humidity for 2014.*

5.4 Wind speed

The behavior of wind speed around the TUT PV power plant will be studied in this section. The measurements have been taken for the year 2014 with an interval of one second between successive measurements. The single average daily value in this case has been calculated from measurements for the time interval 10:00-14:00 hours using the Microsoft Excel computer software. The anemometer used to record the measurements is the ultrasonic WS425 wind sensor. The average daily behavior can be seen in the figure 5.13 below

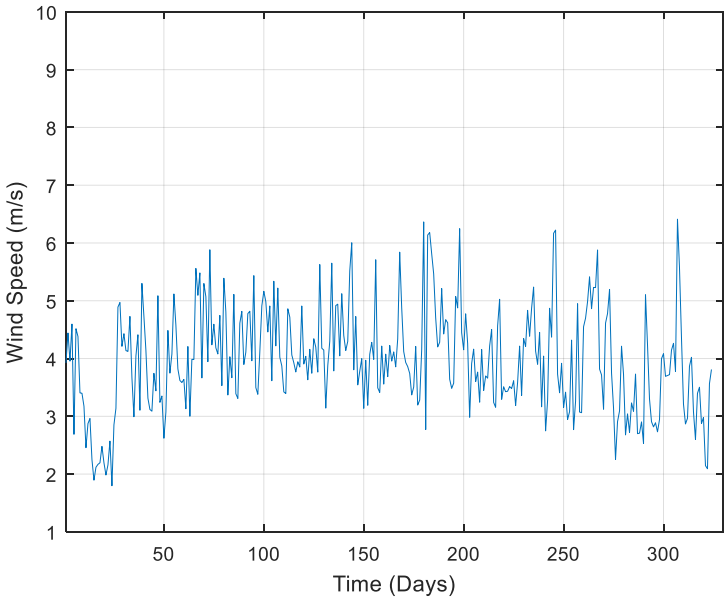

Figure 5.12 *Average daily wind speed profile for 2014.*

Figure 5.13 illustrates that there is a lot of variations in the average wind speed around the PV power plant. The average wind speed fluctuates between 1.798-6.413 m/s. This constant fluctuation makes it very difficult to study and compare the wind speed with other environmental parameters. The seasonal behavior of wind speed makes it easier to analyze. In order to study the seasonal behavior, one month was selected from both each summer and winter. The summer data was taken for August 2014 whereas the winter data was taken from February 2014. The measurement settings were the same as for the annual wind speed profile. The results showed that for most of the days the average wind speed during the month of august was higher than the average wind speed during the month of February. It also confirmed that the average wind speed constantly fluctuates irrespective of any particular season or month. This seasonal behavior of average wind speed can be seen in the figure 5.14.

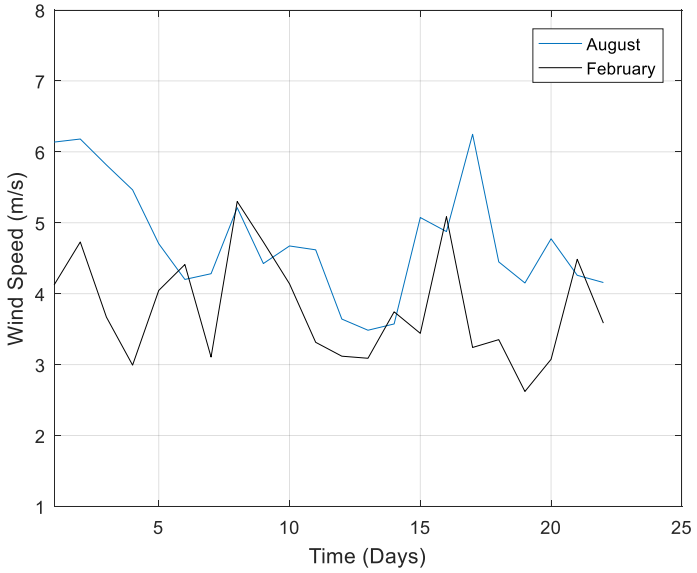

Figure 5.13 *Seasonal average daily wind speed profile for 2014.*

5.5 Module temperature and ambient temperature

Module temperature is the temperature of the PV module receiving the solar irradiance. The TUT solar PV power plant uses the PT100 temperature sensor to measure the module temperature. This sensor is attached to every solar module at the power plant. In this section we will compare the yearly and seasonal profile of the module temperature with that of ambient temperature. For this purpose, the data was taken from the sensors PT18, PT20 and PT21 which are attached to the string of the PV modules located at the highest point of the PV power plant as shown in figure 5.15

Figure 5.14 *PV module string at the highest point of the TUT PV power plant.*

The reason for selecting this particular string was to minimize the effect of shadows in the measurements. The average measurements have been taken for the whole course of the day with a difference of 1 second between successive measurements. It should be noted that some data is not present because of technical problems. The comparison of annual module temperature with the annual ambient temperature can be seen in figure 5.16

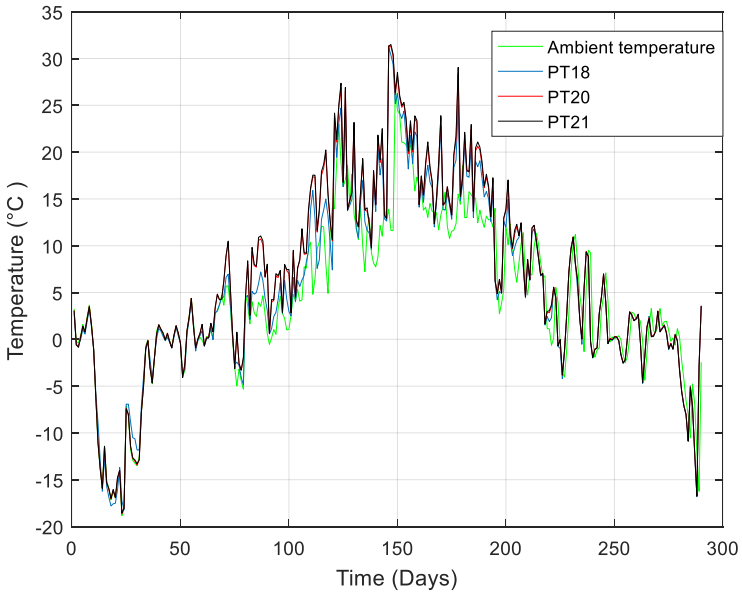

Figure 5.15 *Average daily ambient temperature and average daily module temperature for 2014*

This shows that the module temperature has the same behavior as that of the ambient temperature during the course of the year which means that both these parameters are proportional to each other. The availability of sunlight for longer duration and less cloud cover in the summer allows the PV modules to absorb more sunlight thus increasing the module temperature. However, in winters due to lack of sunlight, heavy cloud cover and snow cover on the PV modules little amount of sunlight is absorbed which results in lower module temperatures. The seasonal profile also confirms this behavior as shown below in figure 5.17. The measurements have been taken for the hottest and coldest month of the year which are August and February respectively with the same settings as in figure 5.16. The average module temperature ranges from -7.054 - 4.056 °C in February whereas in August it ranges from 12 - 31.18 °C

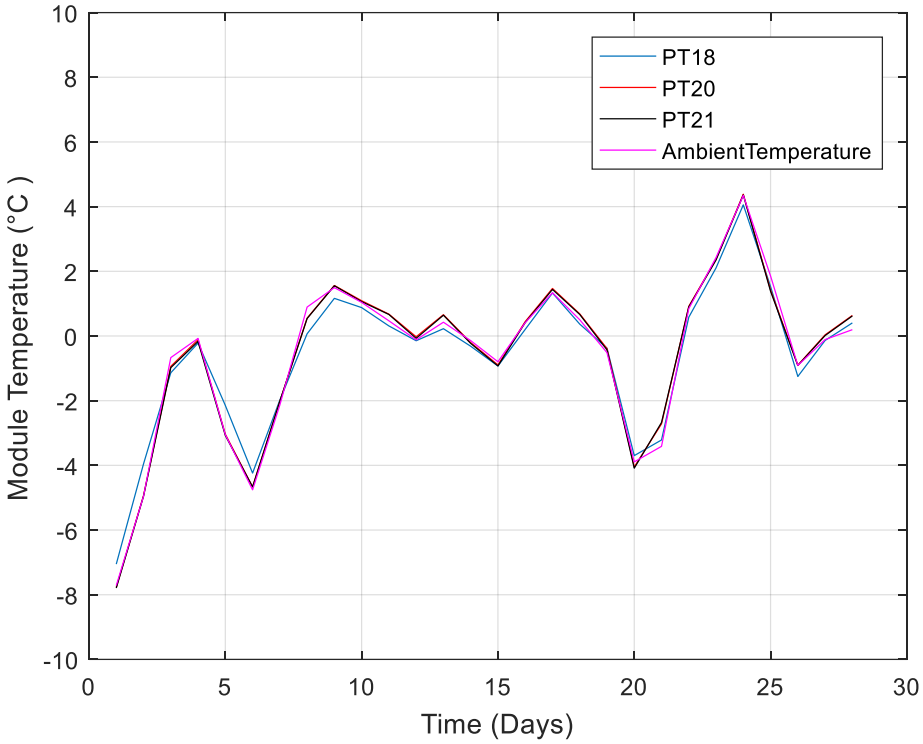

(a)

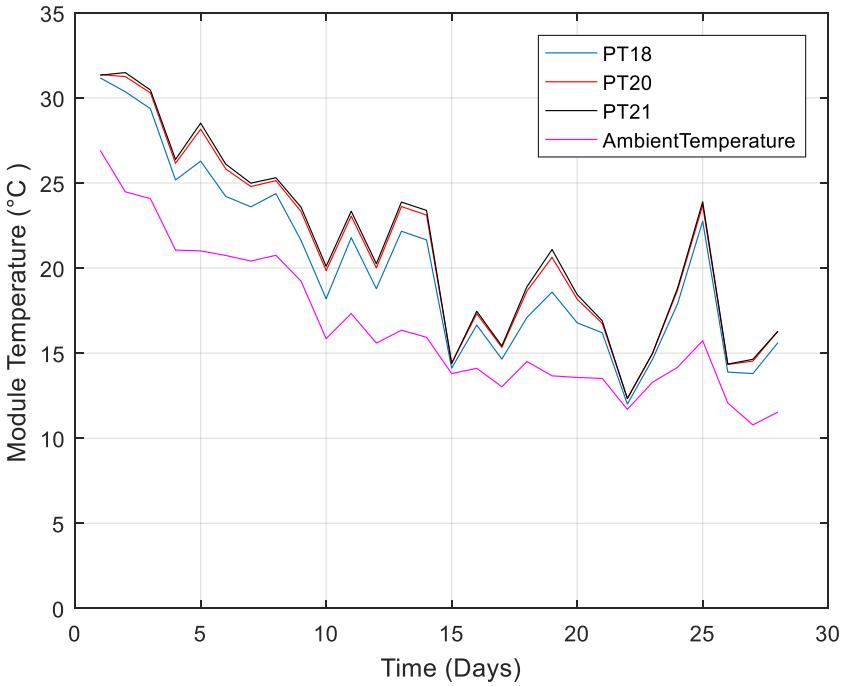

(b)

Figure 5.16 *Seasonal comparison of average daily module temperature and average daily ambient temperature (a)Winter (b)Summer.*

5.6 Module irradiance and global solar radiation

In this section the global solar radiation is compared with the irradiance received by the solar module of a particular string of PV modules. The module solar irradiance data has been measured for the PV string shown in figure 5.15. Data has been measured by the SPlite2 irradiance sensor which can be seen in figure 3.1(a). These sensors are attached individually to the PV modules. In this case data has been taken from the SP18-SP21 sensors for 2014. The data has been calculated for the whole 24-hour course of the day with a difference of one second between successive measurements. The average daily values have been calculated using the Microsoft Excel software. Figure 5.17 shows the comparison of the annual average global solar radiation with the annual average module solar irradiance

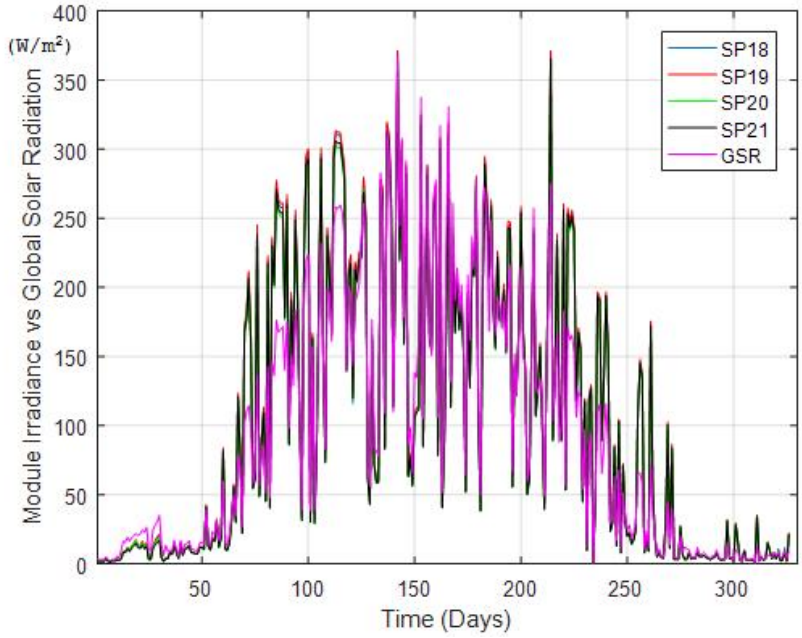

Figure 5.17 *Average daily module solar irradiance and average daily global solar radiation (GSR).*

It can be seen clearly from figure 5.18 that the module irradiance is directly proportional to the global solar radiation. This relationship can further be confirmed by comparing the average module irradiance with average global solar radiation seasonally. Seasonal behavior is the profile of average module irradiance and global solar radiation for the month of February and August 2014 with the former illustrating the winter profile whereas the later depicting the behavior in summer. Figure 5.19 shows this seasonal behavior. Average module irradiance during February fluctuates between 1.926 - 42.88 W/m^2 corresponding to the variation in global solar radiation which varies from 5.278 -

39.85 W/m^2. In august, the average global solar radiation is between 60.02 - 272.3 W/m^2 whereas the average module irradiance is 51.72 - 294.7 W/m^2.

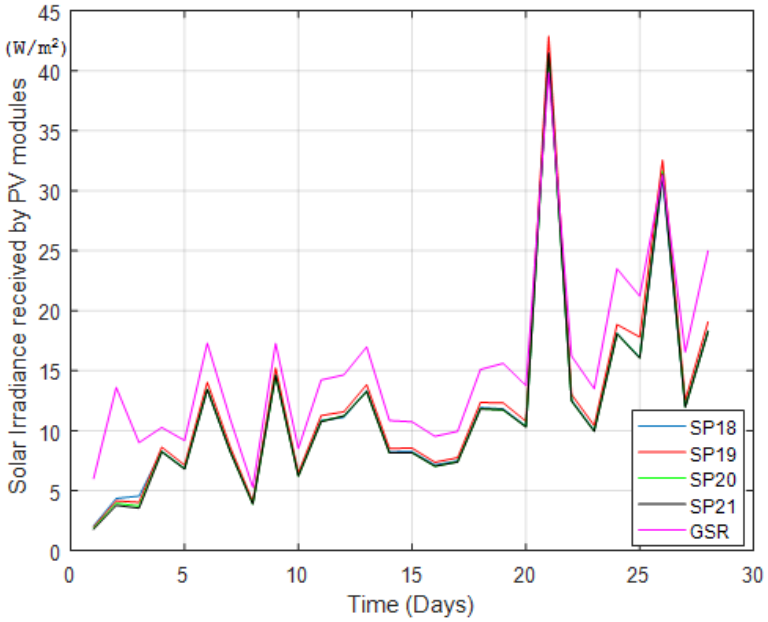

(a)

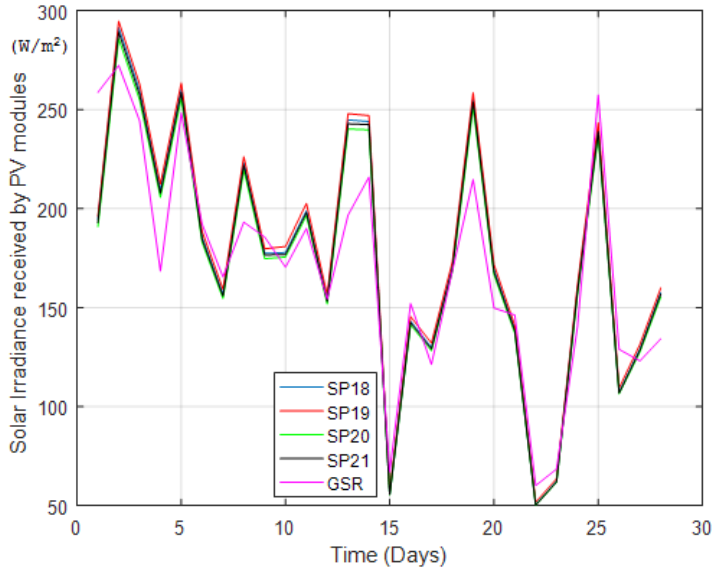

(b)

Figure 5.18 *Seasonal comparison of average daily module irradiance and average daily global solar radiation (a)Winter (b)Summer.*

6. CONCLUSIONS

In chapter 5 the annual and seasonal profiles of various environmental parameters were studied and analyzed for the year 2014. An effort was made to find a correlation between these parameters. In the first section the profiles of the global and diffused solar radiation were studied separately and then they were correlated. The correlation showed that during the winter time the solar irradiance is entirely composed of the diffused solar radiation. The reason for this high percentage of diffused solar radiation is the presence of heavy cloud cover, high percentage of atmospheric humidity and shorter periods of sunlight. Therefore, it is very important to harvest the maximum amount of diffused solar radiation in the winter time.

In the second section the ambient temperature and humidity were studied annually and seasonally for the same year 2014. It was deduced from the ambient temperature profile that during the summer time clear skies and longer sunlight hours resulted in the high values of ambient temperature. Humidity was low during the summer time whereas in the winter time it was high. There was a lot of variation in humidity of the atmosphere during the summer time as compared to that in the winter time. It was deduced from this high variation that the atmospheric conditions vary a lot during the summer time as compared to the winter time when there is almost constant cloud cover. Ambient temperature and humidity were correlated and it was found that the increase in ambient temperature subsequently decreased the humidity or vice versa. The reason for this inverse relationship was that during the summer time clear sky conditions decreased the humidity thus increasing the temperature whereas in the winter time due to the high percentage of clouds in the sky the humidity was high. Humidity was also compared to the global solar radiation and the same relationship was found as it had with the ambient temperature.

It was concluded from the annual and seasonal behavior of wind speed that there was a constant fluctuation in the wind speed around the year. But when the wind speed for the winter was compared to the wind speed for the summer it was found that the average wind speed during summer was higher than the average wind speed during the winter. This seasonal profile also confirmed the fact that the wind speed always fluctuates and is never constant. The behavior of module temperature was found to be in direct correlation with the ambient temperature. The availability of longer sunlight hours during the summer increased the ambient temperature which in turn allowed the PV modules to absorb more sunlight thus increasing the module temperature whereas in the winter when there was almost no direct sunlight and there was snow cover ambient temperature was low which made the absorption of sunlight minimal thus decreasing the PV module temperature. The seasonal behavior confirmed the exact same behavior.

The module irradiance showed the same behavior as the solar irradiance. During the months of summer when the solar irradiance was high the module irradiance was also high whereas in the winter time when the solar irradiance was very low the module irradiance also decreased. The reason for this decrease in module irradiance with the onset of winter is the lack of direct sunlight due to the shorter span of the days. We can conclude from chapter 5 that the TUT PV power plant operates efficiently in the summer months. In the summer due to the higher percentage of global solar radiation the PV modules absorb more sunlight thus increasing the amount of absorbed solar energy. The high percentage of global solar radiation is due to the less amount of cloud cover which subsequently decreases the humidity content in the atmosphere and thus minimizing the diffused solar radiation. In winters the case is completely opposite and the efficiency is very low. But it can be increased by harvesting the maximum amount of diffused solar radiation. This can be achieved by changing the tilt angle of the PV modules. In winter the PV modules shall be placed in a horizontal orientation for maximum absorption of solar radiation.

REFERENCES

[1] Jayakumar, P. Solar energy resource assessment handbook. APCTT, 2009.

[2] International Energy Agency. Solar energy perspectives. 2011. [accessed on 14.04.2016]. Available at: http://tinyurl.com/hjyj7s2

[3] United States Department of Energy. The history of solar. 2012. [accessed on 14.04.2016]. Available at: https://www1.eere.energy.gov/solar/pdfs/solar_timeline.pdf.

[4] Amaripadath, D, Effects of diffuse radiation to the operation of photovoltaic power plants. Master of Science Thesis. Tampere University of Technology. Tampere 2015.

[5] Markvart, T. Solar electricity. United Kingdom 2001, John Wiley and Sons.

[6] Torres Lobera, D, Measuring actual operating conditions of a photovoltaic power generator. Master of Science Thesis. Tampere University of Technology. Tampere 2010.

[7] Häberlin, H. Photovoltaics system design and practice. Switzerland 2010, John Wiley and Sons.

[8] Lappalainen, K, Effects of climate and environmental conditions on the operation of solar photovoltaic generators. Master of Science Thesis. Tampere University of Technology. Tampere 2013.

[9] Sunny, M, Sizing an energy storage to be used in parallel with a PV inverter to balance the fluctuations in output power from PV generator. Master of Science Thesis. Tampere University of Technology. Tampere 2014.

[10] Lynn, P.A. Electricity from Sunlight: An Introduction to Photovoltaics. 2010, John Wiley & Sons Ltd.

[11] Ahola, J, Photovoltaic research power plant measuring and data storing system. Master of Science Thesis. Tampere University of Technology. Tampere 2013.

[12] PN and metal semiconductor junctions. Faculty of Electrical Engineering and Computer Sciences, University of California, Berkeley. 2009. [accessed on 27.04.2016]. Available at: http://www.eecs.berkeley.edu/~hu/Chenming-Hu_ch4.pdf

[13] Valkealahti, S. Solar power systems. Department of Electrical Engineering, Tampere University of Technology, Tampere. 2014.

[14] Mäki, A, Topology of a silicon based grid connected photovoltaic generator. Master of Science Thesis. Tampere University of Technology. Tampere 2010.

[15] Bremner, S. Solar electric systems. Faculty of Electrical and Computer Engineering, University of Delaware, Delaware. 2009. [accessed on 27.04.2016]. Available at: http://www.solar.udel.edu/ELEG620/13_PV_modules.pdf

[16] Eltawil, M.A. and Zhao, Z. Grid-connected photovoltaic power systems: Technical and potential problems—A review. Renewable and Sustainable Energy Reviews 14(2010)1, pp. 112-129.

[17] Torres Lobera, D, Mäki, A, Huusari, J, Lappalainen, K, Suntio, T and Valkealahti, S. Operation of TUT solar PV power station research plant under partial shading caused by snow and buildings. International Journal of Photoenergy, vol 2013. Article ID 837310, 13 pages, 2013.

[18] Campbell Scientific Corp, Canada. User manual for SP Lite2 pyranometer. 2015. [accessed on 13.06.2016]. Available at: https://s.campbellsci.com/documents/ca/manuals/splite2_man.pdf.

[19] World Meteorological Organization. Guide to Meteorological Instruments and Methods of Observation. WMO No. 8, 2008. [accessed on 13.06.2016]. Available at: http://library.wmo.int/pmb_ged/wmo_8-2012_en.pdf

[20] KIPP & ZONEN. KIPP & ZONEN user manual for CMP pyranometers. 2015. [accessed on 13.06.2016]. Available at: www.kippzonen.com/Download/72/Manual-Pyranometers-CMP-series-English.

[21] KIPP & ZONEN. KIPP & ZONEN user manual for CMP 121 shadow ring. [accessed on 13.06.2016]. Available at: www.kippzonen.com/Download/46/CM121-B-C-Shadow-Ring-Manual

[22] VAISALA. VAISALA user manual for HMP155 temperature and humidity sensor. [accessed on 13.06.2016]. Available at: www.vaisala.fi/Vaisala%20Documents/.../HMP155_User_Guide_in_English.pdf

[23] VAISALA. VAISALA user manual for WS425 ultrasonic wind sensor. [accessed on 13.06.2016]. Available at: http://www.vaisala.com/Vaisala%20Documents/User%20Guides%20and%20Quick%20Ref%20Guides/WS425_User_Guide_in_English.pdf

[24] TUT solar photovoltaic power station test plant. [accessed on 27.06.2016]. Available at:
http://www.tut.fi/cs/groups/public/@l813/@web/@p/documents/liit/mdbw/mduy/~edisp/p052294.pdf

[25] Sureshgoud, S and Rao, N. Development of an Integrated Data-Acquisition System for Renewable Energy Sources Systems Monitoring. International Journal & Magazine of Engineering, Technology, Management and Research, vol 1, 2014. pp 630-636.

[26] Archer, M.D. and Hill, R, Clean electricity from photovoltaics. United Kingdom 2001, Imperial College Press.

APPENDIX A: LAYOUT OF TUT SOLAR PV POWER PLANT

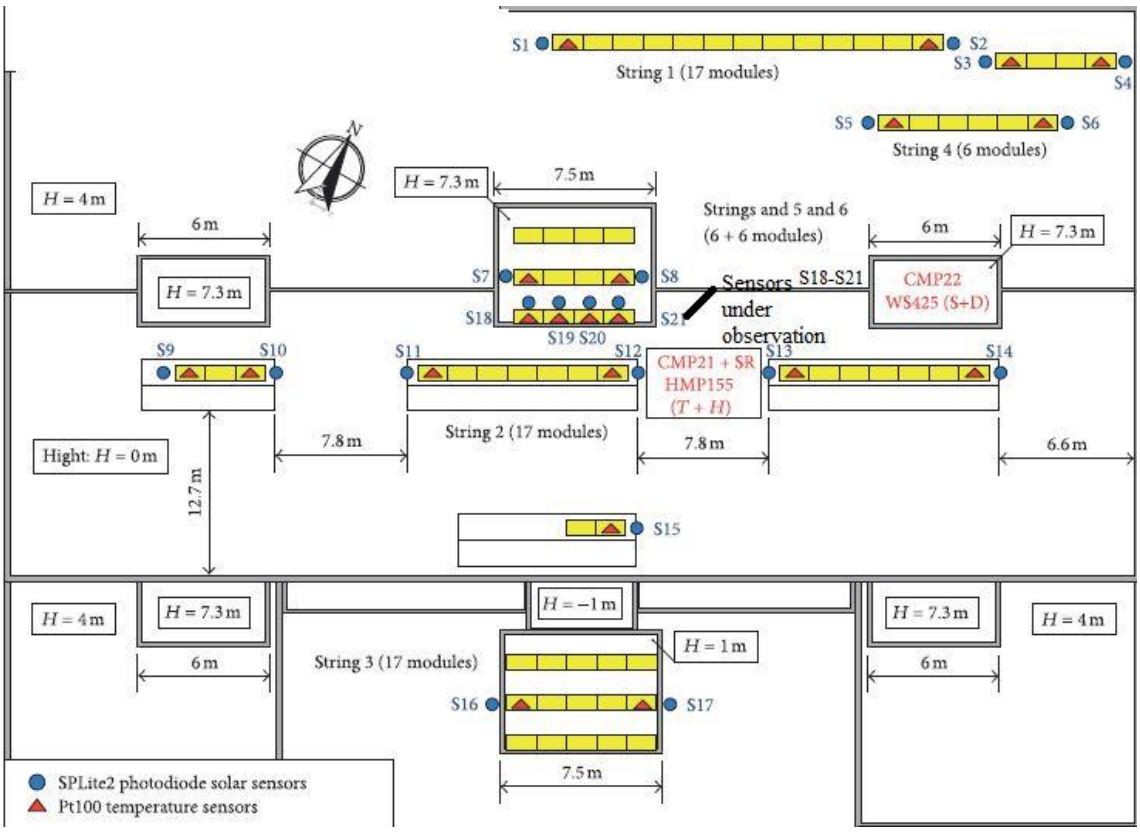

Figure A.1 *TUT solar PV research power plant layout*